ASYMPTOTIC ANALYSIS OF HYPERSONIC VEHICLE DYNAMICS ALONG ENTRY TRAJECTORY

by

William D. Janicki
Lt, United States Air Force
B.S., Astronautical Engineering
U.S. Air Force Academy, 1989

Submitted to the
Department of Aeronautics and Astronautics
in Partial Fulfillment of the Requirements
for the Degree of

Master of Science
at the
Massachusetts Institute of Technology

June 1991

Signature of Author_____
Department of Aeronautics and Astronautics

Approved by_____
Dr. Rudrapatna V. Ramnath, Thesis Supervisor
Professor of Aeronautics and Astronautics, MIT

Certified by_____
Philip Hattis, Technical Supervisor
The Charles Stark Draper Laboratory, Inc.

Accepted by_____
Professor Harold Y. Wachman, Chairman
Departmental Graduate Committee

ASYMPTOTIC ANALYSIS OF HYPERSONIC VEHICLE DYNAMICS ALONG ENTRY TRAJECTORY

by

William D. Janicki
Lt, United States Air Force

Submitted to the Department of Aeronautics and Astronautics
on May 20, 1991 in partial fulfillment of the requirements for the
Degree of Master of Science in Aeronautics and Astronautics

ABSTRACT

The dynamics of a hypersonic vehicle (HSV) along an entry trajectory were analyzed using the asymptotic method of Generalized Multiple Scales (GMS). A mathematical model describing the expected performance of future HSVs was provided by NASA called the Generic Hypersonic Aerodynamic Model Example (GHAME). This model was used for computer simulation of flight along an entry trajectory which is flown by the Space Shuttle. The characteristic modes of motion of the GHAME vehicle are recorded, and the equations of motion are analyzed through the GMS technique.

The results show that the analytical solutions to the equations of aircraft motion developed by the GMS technique closely approximate the numerical solutions. From these results, the approximations are shown to be valid for stability and control analysis. A stability criterion for the modes of the GHAME vehicle was established and a feedback controller was designed to stabilize an unstable mode.

Thesis Supervisor: Dr. Rudrapatna V. Ramnath
Professor of Aeronautics and Astronautics, MIT

ACKNOWLEDGEMENTS

This report was prepared at The Charles Stark Draper Laboratory. It was supported in part by the Independent Research and Development project *Hypervelocity Vehicle Data Collection System and Avionics Design Characterization* (IR&D 300). Partial support is also acknowledged from NASA Dryden Flight Research Facility through Vimanic Systems and Professor Rudrapatna V. Ramnath. Publication of this report does not constitute approval by the Charles Stark Draper Laboratory or the Massachusetts Institute of Technology of the findings or conclusions contained herein. It is published solely for the exchange and stimulation of ideas.

TABLE OF CONTENTS

TABLE OF FIGURES

TABLE OF TABLES

1. INTRODUCTION

HYPERSONIC FLIGHT

The technology related to hypersonic vehicles (HSVs) has been given increased attention in recent years. HSVs are aerospace vehicles designed to fly at speeds in excess of Mach 6 and have air breathing propulsion systems. Now that the Space Shuttle is operational, research interest has turned to the development of other reusable space transportation systems as long term alternative shuttle-like vehicles. These systems would provide additional operational capabilities such as increased maneuverability within the atmosphere, lower cost of payload to orbit, quicker turnaround time and less ground support. This technology, which has many military as well as civilian applications, will be demonstrated by the proposed National Aerospace Plane (NASP). In order to develop HSVs, research is required to increase the knowledge base of these vehicles.

The NASP is a single stage-to-orbit horizontal take-off and landing vehicle expected to fly at approximately Mach 25. Research related to this vehicle is currently being conducted at a number of facilities throughout the government and private industry. Although high speed atmospheric trajectories such as that flown by the Space Shuttle have provided much relevant data on hypersonic flight, these trajectories provide limited information regarding the NASP because of the restricted shuttle flight envelope. This leaves much additional research to assure success of the NASP. Remaining research includes hypersonic propulsion systems, guidance and control systems, air data measurement systems and airframe

design. These systems are interrelated so that the design of one affects the design of others.

An understanding of the fundamental dynamics of HSVs along high speed atmospheric trajectories is critical to the overall vehicle design and integration of its various subsystems. This thesis attempts to gain insight into the dynamics of an HSV along an entry trajectory. A mathematical model is used which simulates the expected performance of future HSVs. It was provided by NASA and called the Generic Hypersonic Aerodynamic Model Example (GHAME). This model is used for computer simulation of flight along a nominal re-entry trajectory and the aircraft equations of motion are computed at discrete points along the trajectory. The equations of motion are analyzed using the technique of Generalized Multiple Scales (GMS) developed by Rudrapatna Ramnath on the principles of asymptotic analyses [11-14].

ASYMPTOTIC ANALYSIS

The equations of aircraft motion result in a series of linear differential equations with variable coefficients. It is impossible to obtain exact solutions of such equations except in rare cases. Therefore, approximate methods of solution are used to understand the dynamics of the system. A broad class of approximations use perturbation methods to give an approximate solution in closed analytical form.

Asymptotic analysis deals with the limiting behavior of functions that arise as solutions to mathematical models such as differential equations. Functions are considered to be dependent upon variables and parameters. The method of asymptotic expansions is based on the idea of

expansion of the unknown solution $f(x,\varepsilon)$ in a series of powers of some small parameter ε and grouping like powers of the parameter to develop solutions. The power series are normally divergent, yet the approximate solutions can be obtained by cutting off the formal series at some finite term [5]. Convergent series may not always be practical computationally. Asymptotic series give the ability to compute the solution with only a small number of terms.

The approximate solutions obtained in this way are asymptotic to the exact solution. Instead of tending to the exact solution with increasing number of terms, the approximate solution approaches the exact solution as the small parameter tends to zero. Greater accuracy is obtained by considering higher powers of ε. However, this direct perturbation method leads to difficulties especially in the study of dynamic systems. The approximations fail to yield uniformly accurate solutions in many cases. As terms are added to the approximation, the solution may improve in one region but degrade in accuracy in another region. These nonuniformities lead to the development of the technique of Generalized Multiple Scales in order to obtain uniformly accurate asymptotic approximations to the solutions of differential equations.

Asymptotic expansions have their origins in the 18th century in the work of Euler and Laplace, who employed divergent series approximations [5]. Asymptotic representations of solutions to differential equations were already present in the works of Liouville (1837), Green (1837) and Stokes (1848) [8]. However, for much of the 19th century these methods were largely ignored because of the concentration on rigorous mathematical analysis. It was not until the rigorous definition of asymptotic expansions

by Poincare' (1886) that they were used to approximate solutions to ordinary differential equations [5].

Asymptotic approximations developed rapidly in problems such as those encountered in mathematical physics as well as practical problems such as projectile motion. Poincare' applied direct perturbation methods to his research in celestial mechanics. The work done by Birkhoff (1908) generalized asymptotic results to *n*th order and for systems of equations [5]. The work by Pugachev in the period 1940-46 related the theory of asymptotic representations of solutions of nonhomogeneous ordinary differential equations of second and higher order whose coefficients contained a parameter [8]. Kylov and Bogoliubov developed asymptotic methods for the solutions to problems in nonlinear mechanics [8]. Ramnath continued the work of asymptotic expansions with the development of the Generalized Multiple Scales method which gives uniformly valid approximate solutions to linear and nonlinear differential equations with variable coefficients.

PROJECT OVERVIEW

In this thesis, the Generalized Multiple Scales method of asymptotic approximation developed by Ramnath [11-14] is applied to investigate the dynamics of the Generic Hypersonic Aerodynamic Model Example (GHAME) along a nominal entry trajectory. The research deals with asymptotic approximations to solutions of linear differential equations in which the coefficients are a function of a slow time parameter. This indicates that the coefficients of the equation vary slowly; their derivatives with respect to the independent variable are proportional to the small parameter.

Chapter Two presents the general equations of aircraft motion. The aerodynamic axes and parameters are defined, rigid body dynamics are reviewed, and the aircraft dynamics are separated into longitudinal and lateral-directional motion. Small disturbance theory is employed to arrive at nondimensional perturbation equations of motion. Finally, the aerodynamic forces, moments and stability derivatives are calculated.

Chapter Three describes the general modes of aircraft motion and reviews the general types of dynamic solutions to characteristic equations. Typical root locations for longitudinal and lateral-directional modes of motion are also presented. Chapter Four describes the GHAME aerodynamic model to include the vehicle description, mass properties and presentation of aerodynamic data. The entry trajectory to be flown by the GHAME vehicle is described in Chapter Five. The guidance concept is described, the vehicle constraints and interface conditions are presented, and the nominal values of trajectory parameters are plotted.

Chapter Six presents the Generalized Multiple Scales technique of asymptotic approximations. The development of the method is reviewed, and the technique is applied to the unified angle of attack equation developed by Vinh and Laitone [15]. Chapter Seven describes the simulation of the GHAME vehicle along the entry trajectory. The root locations of the equation describing the unified angle of attack dynamics as well as those describing longitudinal and lateral-directional motion are presented. The solutions to the GHAME equations of motion are presented in Chapter Eight. Numerical solutions are determined for each mode of motion and compared to "frozen" approximations with constant coefficients. The GMS solutions are then compared with the numerical solutions and conclusions are drawn. Chapter Nine applies the GMS solutions to the

analysis of stability and control. A stability criterion is determined based on the GMS solutions, and a feedback controller is designed to stabilize an unstable mode. The highlights of the thesis are summarized in Chapter Ten and conclusions are drawn as to the validity and application of the GMS asymptotic solutions to the GHAME equations of motion.

2. EQUATIONS OF AIRCRAFT MOTION

INTRODUCTION

An airplane in flight is a complicated dynamic system. To describe its motion it is necessary to define a suitable coordinate system to formulate the equations of motion. The aircraft is assumed to be a single rigid body. The equations of motion are developed through the application of Newton's second law for both translational and rotational dynamics. The summation of the external forces on the airplane describe the translational motion of the center of mass, while the summation of the external moments describe the rotational motion of the airplane.

The equations derived from Newton's second law are linearized using small-disturbance theory. The aerodynamic forces and moments are also linearized. The resulting equations are nondimensionalized for generality and separated into those describing longitudinal motion and those describing lateral-directional motion.

AXES AND NOTATION

Two coordinate systems are used to describe aircraft dynamics. One coordinate system is fixed to the earth and is considered to be an inertial frame of reference. The other is fixed to the aircraft and rotates with it. Both frames of reference are orthogonal right hand rule coordinate systems. The principle axes used to define the forces and moments acting on the aircraft are fixed to the airplane with origin at the center of mass and move with the airplane. The X axis passes out the nose

of the aircraft, the Y axis passes out the right wing and the Z axis passes through the bottom. The XZ plane is the plane of symmetry. Figure 2.1 shows the aircraft axis system and Table 2.1 defines the aerodynamic parameters.

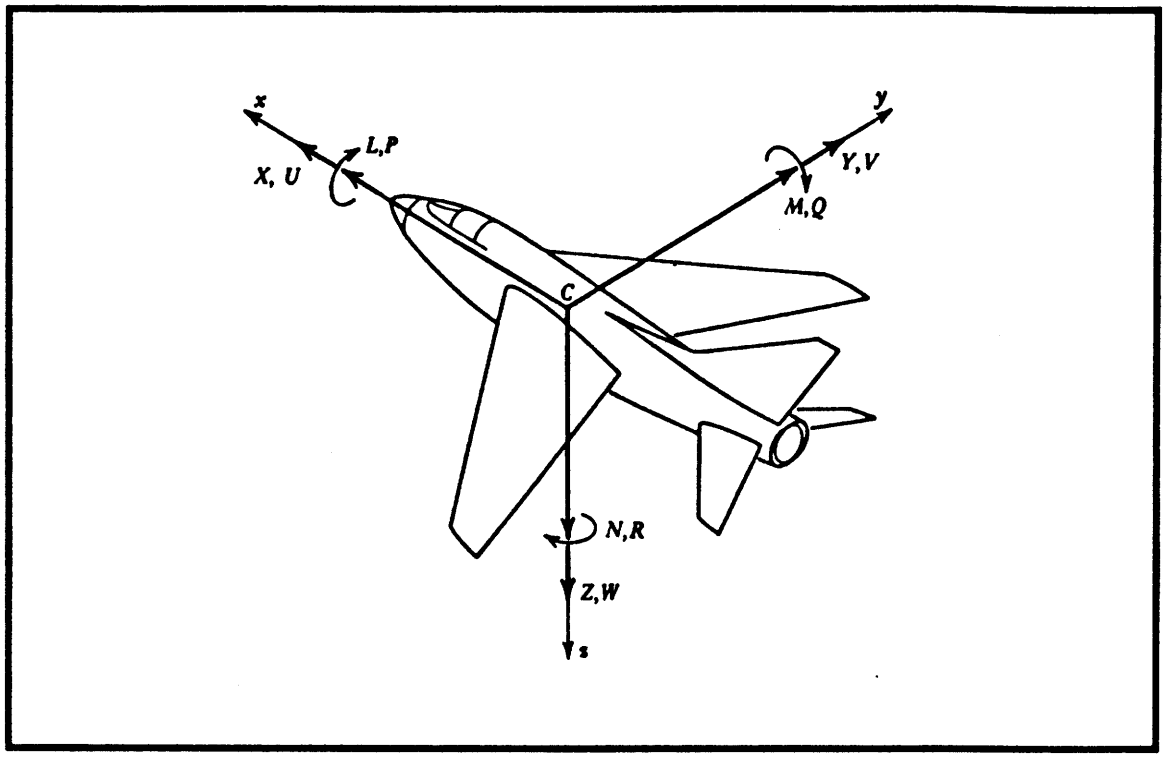

Figure 2.1 - Aircraft Body Fixed Axes and Notation

Parameter	Roll Axis X	Pitch Axis Y	Yaw Axis Z
Velocity Component	u	υ	w
Aerodynamic Force Component	x	y	z
Angular Rates	P	Q	R
Aerodynamic Moment Component	L	M	N
Angular Displacement	ϕ	θ	ψ
Moment of Inertia	I_{xx}	I_{yy}	I_{zz}

Table 2.1 - Aerodynamic Parameters in Body Fixed Coordinates

The position and orientation of the aircraft cannot be described using the body fixed frame of reference alone because it moves with the aircraft. Therefore, the inertial coordinate system fixed to the earth is used. The body fixed angular velocity vector describes the rotation of the body fixed axes with respect to the inertial frame of reference. From this relation the position and orientation of the aircraft can be determined.

The angle of attack (α) is the angular difference between the X axis and the wind velocity vector in the XZ plane. This is positive when the wind velocity vector is between the positive X axis and the positive Z axis. The angle of side slip (β) is the angle between the wind velocity vector and the XZ plane. This is positive when the wind velocity vector is between the positive X axis and the positive Y axis. The flight path angle (γ) is the difference between the angle of attack and the pitch angle.

$$\alpha = \tan^{-1}(w/u) \qquad \beta = \sin^{-1}(\upsilon/v) \qquad \gamma = \alpha - \theta$$

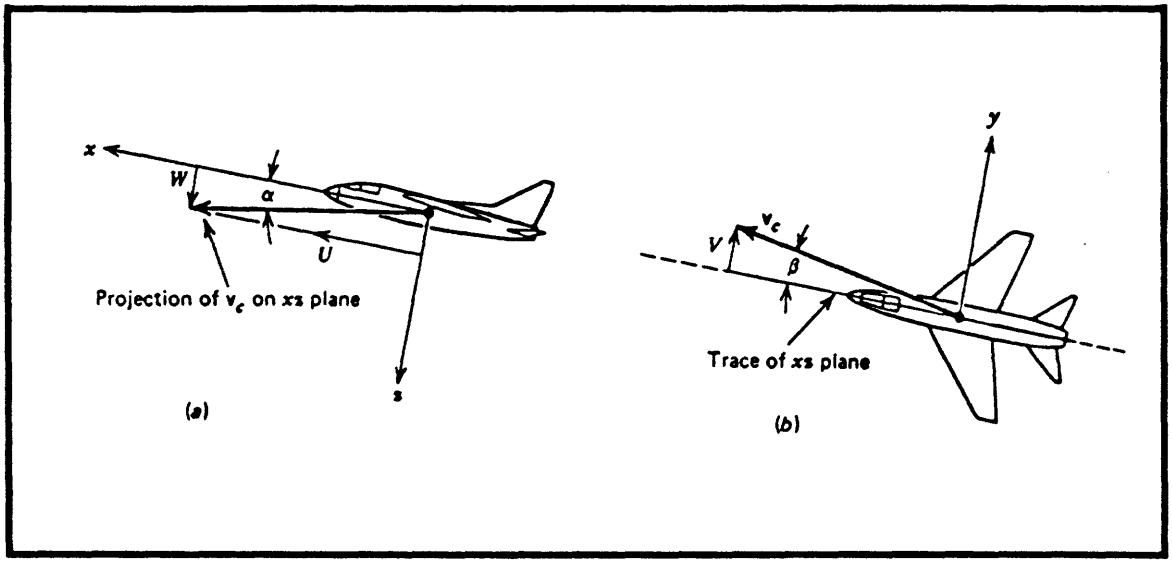

Figure 2.2 - (a) Definition of α. (b) Definition of β

RIGID BODY EQUATIONS OF MOTION

The rigid body equations of motion are obtained from Newton's second law which states that the summation of all external forces acting on the body is equal to the time rate of change of linear momentum (mv) of the body, and the summation of the external moments acting on the body is equal to the time rate of change of angular momentum (H). Newton's second law is expressed in the vector equations

(linear momentum equation)

$$\Sigma F = \frac{d}{dt}(mv)$$

and

(angular momentum equation)

$$\Sigma M = \frac{d}{dt}(H)$$

The vector equations can be rewritten in scalar form as three force equations and three moment equations. The force equations are

$$F_X = \frac{d}{dt}(mu) \qquad F_Y = \frac{d}{dt}(mv) \qquad F_Z = \frac{d}{dt}(mw)$$

The forces are composed of contributions due to the aerodynamic, propulsive, and gravitational forces acting on the aircraft. The moment equations are

$$M_X = \frac{d}{dt}(H_x) \qquad M_Y = \frac{d}{dt}(H_y) \qquad M_Z = \frac{d}{dt}(H_z)$$

The moments and products of inertia are defined as

$$I_{xx} = \iiint (y^2 + z^2)dm \qquad I_{xy} = \iiint xydm$$

$$I_{yy} = \iiint (x^2 + z^2)dm \qquad I_{xz} = \iiint xzdm$$

$$I_{zz} = \iiint (x^2 + y^2)dm \qquad I_{yz} = \iiint yzdm$$

If the reference frame is not rotating then the moments and products of inertia will vary with time as the aircraft rotates. To avoid this, the axis system is fixed to the aircraft. The moments and products of inertia are then constant.

The derivation of the equations of aircraft motion can be seen in Nelson's Flight Stability and Automatic Control [7]. The resulting equations are presented below.

Translation:

$$F_X = m(\dot{u} + qw - rv)$$

$$F_Y = m(\dot{v} + ru - pw)$$

$$F_Z = m(\dot{w} + pv - qu)$$

Rotation:

$$L = \dot{H}_X + qH_Z - r H_Y$$

$$M = \dot{H}_Y + rH_X - pH_Z$$

$$N = \dot{H}_Z + pH_Y - qH_X$$

The XZ plane is the plane of symmetry so the products of inertia I_{yz} and I_{xy} go to zero. The moment equations can then be written as

$$L = I_{xx}\dot{p} - I_{xz}\dot{r} + qr(I_{zz} - I_{yy}) - I_{xz}pq$$

$$M = I_{yy}\dot{q} + rp(I_{xx}-I_{zz}) + I_{xz}(p^2 - r^2)$$

$$N = -I_{xz}\dot{p} + I_{zz}\dot{r} + pq(I_{yy}-I_{xx}) + I_{xz}qr$$

LONGITUDINAL AND LATERAL-DIRECTIONAL MOTION

Because of the existence of a plane of symmetry the equations of motion can be divided into longitudinal motion and lateral-directional motion. Longitudinal motion occurs in the plane of symmetry. This consists of translation along the flight path, translation perpendicular to

the flight path and rotation about the Y axis. The lateral-directional motion occurs outside the plane of symmetry. This includes translation along the Y axis, roll rotation and yaw rotation. The longitudinal force diagram is presented in Figure 2.3.

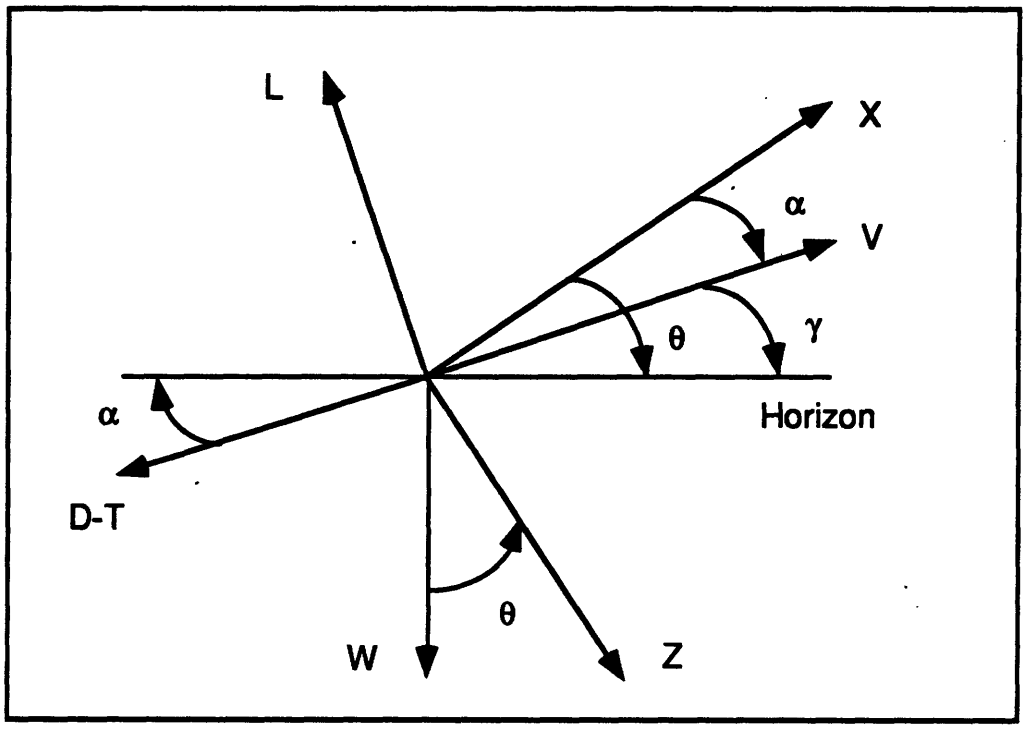

Figure 2.3 Longitudinal Force Diagram of Aircraft in Flight

The lift vector is perpendicular to the flight path (v). The drag vector is opposite the flight path and perpendicular to the lift vector. The aerodynamic force in the X direction is given by

$$X = L\sin\alpha - (D-T)\cos\alpha$$

The aerodynamic force in the Z direction is given by

$$Z = -L\cos\alpha - (D-T)\sin\alpha$$

The lateral-directional force diagram is presented in Figure 2.4. The gravitational force acts through the center of mass and contributes to the

external force acting on the aircraft. It can be seen from the force diagrams to have components along each of the body axes. It will not,

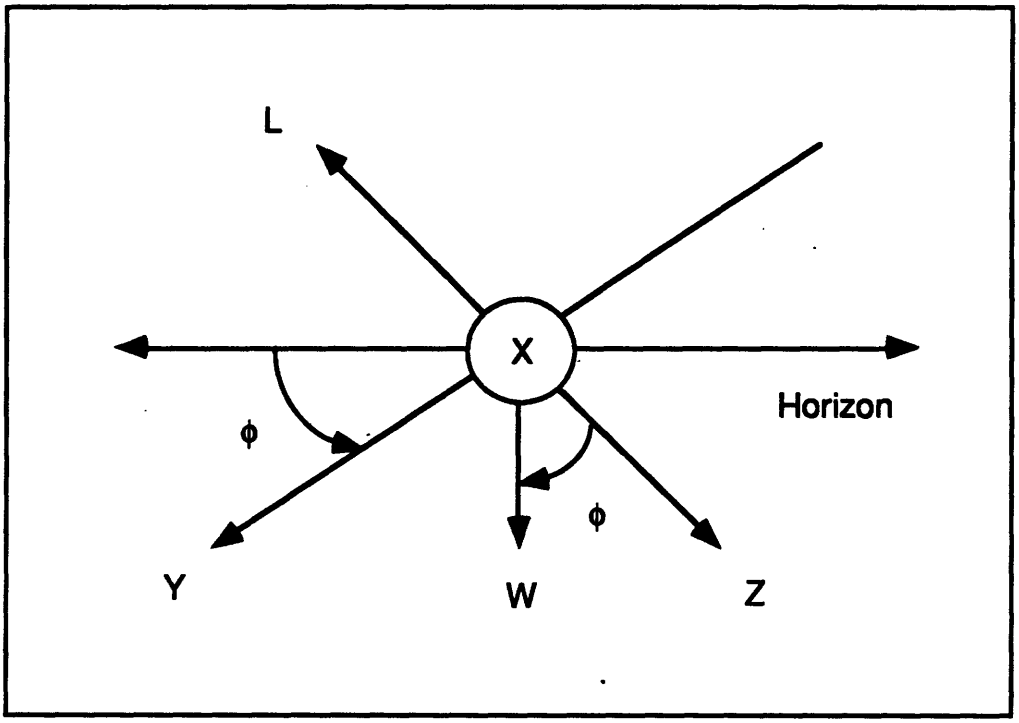

Figure 2.4 Lateral-Directional Force Diagram of Aircraft in Flight

however, produce any moments because it acts through the mass center.

$$F_X \text{ gravity} = -\, mg \sin\theta$$

$$F_Y \text{ gravity} = mg \cos\theta \sin\phi$$

$$F_Z \text{ gravity} = mg \cos\theta \cos\phi$$

The components of gravity are included in the equations of motion, and the resulting equations are summarized in Table 2.2 [7].

Force Equations	Moment Equations
$X - mg\sin\theta = m(\dot{u} + qw - rv)$	$L = I_{xx}\dot{p} - I_{xz}\dot{r} + qr(I_{zz} - I_{yy}) - I_{xz}pq$
$Y + mg\cos\theta\sin\phi = m(\dot{v} + ru + pw)$	$M = I_{yy}\dot{q} + rp(I_{xx}-I_{zz}) + I_{xz}(p^2 - r^2)$
$Z + mg\cos\theta\cos\phi = m(\dot{w} + pv - qu)$	$N = -I_{xz}\dot{p} + I_{zz}\dot{r} + pq(I_{yy}-I_{xx}) + I_{xz}qr$

Table 2.2 - Summary of Aircraft Equations of Motion

SMALL DISTURBANCE THEORY

The equations of motion are linearized for stability and control analysis by assuming that the motion of the airplane consists of small deviations from a reference steady state condition. The details of this derivation are shown in Nelson's text, and the highlights are presented here [7]. All the variables in the equations of motion are replaced by a reference value plus a perturbation or disturbance.

The reference flight condition is defined where there are no external forces or moments acting on the aircraft. Only first order disturbance terms are kept because they are assumed to be small such that products and squares of the perturbations go to zero. The perturbation X force equation of motion is represented as

$$\Delta X - mg\Delta\theta\cos\theta_0 = m\Delta\dot{u}$$

The equation can be further simplified by expanding the change in the X force in a Taylor series in terms of the perturbation variables. Assuming that ΔX is only a function of u and α it can be expanded as

$$\Delta X = \frac{\partial X}{\partial u}\Delta u + \frac{\partial X}{\partial \alpha}\Delta\alpha + \frac{\partial^2 X}{2\partial u^2}\Delta u^2 + \frac{\partial^2 X}{2\partial \alpha^2}\Delta\alpha^2 + \frac{\partial^2 X}{\partial u \partial \alpha}\Delta u\Delta\alpha$$

The perturbation is linearized by neglecting the higher order terms. This is valid if the disturbances are small. The quantities

$$\frac{\partial X}{\partial u} \qquad \frac{\partial X}{\partial \alpha}$$

are called stability derivatives and are evaluated at the reference flight condition. After rearranging, the equation becomes

$$(m\frac{d}{dt} - \frac{\partial X}{\partial u})\Delta u - \frac{\partial X}{\partial \alpha}\Delta\alpha + mg\cos\theta_0\Delta\theta = 0$$

The equation is further generalized by making it nondimensional. This is done by dividing through by the mass.

$$(s - X_u)\Delta u - X_\alpha \Delta\alpha + g\cos\theta_0 \Delta\theta = 0$$

where

$$X_u = \frac{\partial X}{\partial u}\frac{1}{m} \qquad X_\alpha = \frac{\partial X}{\partial \alpha}\frac{1}{m} \qquad s = \frac{d}{dt}$$

The remaining equations of motion are developed in a similar way. The moment equations are nondimensionalized by dividing through by the moment of inertia. The resulting perturbation equations of motion are described by six linear differential equations. They are derived by Nelson and presented in Table 2.3 [7].

LONGITUDINAL EQUATIONS
1. $(s - X_u)\Delta u - X_\alpha \Delta\alpha + (g\cos\theta_0)\Delta\theta = 0$
2. $-Z_u \Delta u + (s - Z_\alpha)\Delta\alpha - (su - g\sin\theta_0)\Delta\theta = 0$
3. $-M_u \Delta u - (M_{\dot\alpha} s + M_\alpha)\Delta\alpha + (s - M_{\dot\theta})s\Delta\theta = 0$
LATERAL-DIRECTIONAL EQUATIONS
1. $(s - Y_v)\Delta v + (u - Y_r)\Delta r - (g\cos\phi_0\cos\theta_0)\Delta\phi = 0$
2. $-L_v \Delta v + (\frac{I_{xz}}{I_{xx}} s - L_r)\Delta r + (s^2 - L_p s)\Delta\phi = 0$
3. $N_v \Delta v + (s - N_r)\Delta r - (\frac{I_{xz}}{I_{zz}} s - N_p)\Delta\phi = 0$

Table 2.3 - Nondimensional Perturbation Equations of Motion

The longitudinal equations are made useful for simulation by expressing the X and Z forces in terms of lift and drag and simplifying the equations by assuming that

$$\theta_0 = 0 \rightarrow \cos\theta_0 = 1 \quad \text{and} \quad \sin\theta_0 = 0$$

The X and Z force equations then become

$$(s + c_1D_u - c_2L_u)\Delta u + (c_1D_\alpha - c_2L_\alpha)\Delta\alpha + g\Delta\theta = 0$$

$$(\frac{c_1L_u}{u} + \frac{c_2D_u}{u})\Delta u + (s + \frac{c_1L_\alpha}{u} + \frac{c_2D_\alpha}{u})\Delta\alpha - s\Delta\theta = 0$$

where $c_1 = \cos\alpha$ and $c_2 = \sin\alpha$.

CALCULATION OF AERODYNAMIC FORCES, MOMENTS AND STABILITY DERIVATIVES

The three aerodynamic forces acting on an aircraft are lift, drag and side force. These forces are determined from aerodynamic coefficients by the following equations.

Lift: $L = qSC_L$

$$C_L = C_{L0} + C_{L\alpha}\alpha + C_{Lq}qc_{mac}/2u$$

Drag: $D = qSC_D$

$$C_D = C_{D0} + C_{D\alpha}\alpha$$

Side Force: $Fy = qSC_Y$

$$C_Y = C_{Y0} + C_{Y\beta}\beta + C_{YP}P(b/2u) + C_{YR}R(b/2u)$$

where

q = dynamic pressure = $\rho u^2/2$

S = wing aerodynamic reference area

b = wing aerodynamic reference span

c_{mac} = wing aerodynamic reference chord

The moments acting on the aircraft are defined as torques about the principle axes and include rolling moment, pitching moment and yawing moment. These moments are calculated from aerodynamic coefficients by the following equations.

Rolling moment: $L = qSbC_l$

$$C_l = C_{l0} + C_{l\beta}\,\beta + C_{lP}\,P(b/2u) + C_{lR}\,R(b/2u)$$

Pitching moment: $M = qSc_{mac}C_M$

$$C_M = C_{M0} + C_{M\alpha}\,\alpha + C_{Mq}\,q(c_{mac}/2u)$$

Yawing moment: $N = qSbC_n$

$$C_n = C_{n0} + C_{n\beta}\,\beta + C_{nP}\,P(b/2u) + C_{nR}\,R(b/2u)$$

The linearized equations of aircraft motion can be expressed in terms of stability derivatives. These derivatives represent the changes in aerodynamic forces and moments due to small changes in the perturbation variables. As an example, the α derivatives describe the changes that take place in the forces and moments when the angle of attack is increased. This normally results in an increase in lift, an increase in drag and a negative pitching moment [7]. The stability derivatives are defined in terms of partial derivatives and expressed in terms of elementary aerodynamic parameters for simulation. The D_u derivative is derived below [9].

$$D_u \equiv \frac{\partial D}{\partial u}\frac{1}{m} \qquad D = \frac{1}{2}\rho u^2 S C_D$$

$$\frac{\partial D}{\partial u} = \rho u S C_D \qquad D_u = \frac{\rho u S C_D}{m}$$

This expression gives the value at the equilibrium point of the stability derivative D_u in terms of elementary aerodynamic parameters that can be readily measured. The remaining stability derivatives are evaluated in similar manner and the results are presented in Table 2.4 [9].

Stability derivative	Definition	Expression
D_u	$\frac{\partial D}{\partial u}\frac{1}{m}$	$\frac{\rho u S C_D}{m}$
D_α	$\frac{\partial D}{\partial \alpha}\frac{1}{m}$	$\frac{\rho u S C_{D\alpha}}{m}$
L_u	$\frac{\partial L}{\partial u}\frac{1}{m}$	$\frac{\rho u S C_L}{m}$
L_α	$\frac{\partial L}{\partial \alpha}\frac{1}{m}$	$\frac{\rho u S C_{L\alpha}}{m}$
M_u	$\frac{\partial M}{\partial u}\frac{1}{I_{yy}}$	0
M_α	$\frac{\partial M}{\partial \alpha}\frac{1}{I_{yy}}$	$\frac{\rho u^2 S c_{mac}}{2I_{yy}} C_{M\alpha}$
$M_{\dot{\alpha}}$	$\frac{\partial M}{\partial \dot{\alpha}}\frac{1}{I_{yy}}$	0
$M_{\dot{\theta}}$	$\frac{\partial M}{\partial \dot{\theta}}\frac{1}{I_{yy}}$	$\frac{\rho u S c_{mac}^2}{4I_{yy}} C_{Mq}$
Y_υ	$\frac{\partial Y}{\partial \upsilon}\frac{1}{m}$	$\frac{g}{uC_L} C_{y\beta}$
L_υ	$\frac{\partial L}{\partial \upsilon}\frac{1}{I_{xx}}$	$\frac{\rho v S}{2I_{xx}} C_{l\beta}$
L_r	$\frac{\partial L}{\partial r}\frac{1}{I_{xx}}$	$\frac{\rho u S b^2}{4I_{xx}} C_{lr}$
L_p	$\frac{\partial L}{\partial p}\frac{1}{I_{xx}}$	$\frac{\rho u S b^2}{4I_{xx}} C_{lp}$
N_υ	$\frac{\partial N}{\partial \upsilon}\frac{1}{I_{zz}}$	$\frac{\rho u S b}{2I_{zz}} C_{n\beta}$
N_r	$\frac{\partial N}{\partial r}\frac{1}{I_{zz}}$	$\frac{\rho u S b^2}{4I_{zz}} C_{nr}$
N_p	$\frac{\partial N}{\partial p}\frac{1}{I_{zz}}$	$\frac{\rho u S b^2}{4I_{zz}} C_{np}$

Table 2.4 - Stability Derivatives

3. GENERAL MODES OF AIRCRAFT MOTION

INTRODUCTION

The equations of motion derived earlier describe the stability of an aircraft due to small perturbations from a reference steady state condition. The equations are separated into two independent groups describing longitudinal stability and lateral-directional stability. At any point along the trajectory of a moving aircraft, the flight conditions can be frozen and its stability can be described by these equations. Under frozen flight conditions, the equations are fourth order, ordinary, linear, differential equations with constant coefficients. The solutions to such equations are always exponential in form. For example, the solution for angle of attack (α) perturbations is of the form

$$\alpha = a_1 e^{\lambda_1 t} + a_2 e^{\lambda_2 t} + a_3 e^{\lambda_3 t} + a_4 e^{\lambda_4 t}$$

where $\lambda_1, \lambda_2, \lambda_3, \lambda_4$ are roots of the characteristic equation. The exponential solution will continue to grow when λ is a positive real number and will decay toward zero when it is a negative real number. Complex roots always appear in conjugate pairs and result in solutions that have oscillations. Table 3.1 lists the possible kinds of roots to the characteristic equation and gives their corresponding types of solutions [7].

The motion corresponding to each real root or each complex pair is called a natural mode. Figure 3.1 illustrates the types of solutions corresponding to the various types of modes [7].

Root	Type of Solution
A. Real - Positive	Nonoscillatory / Unstable
B. Real - Negative	Nonoscillatory / Stable
C. Complex - Positive Real Part	Oscillatory / Unstable
D. Complex - Negative Real Part	Oscillatory / Stable

Table 3.1 - Possible Roots and Corresponding Solutions

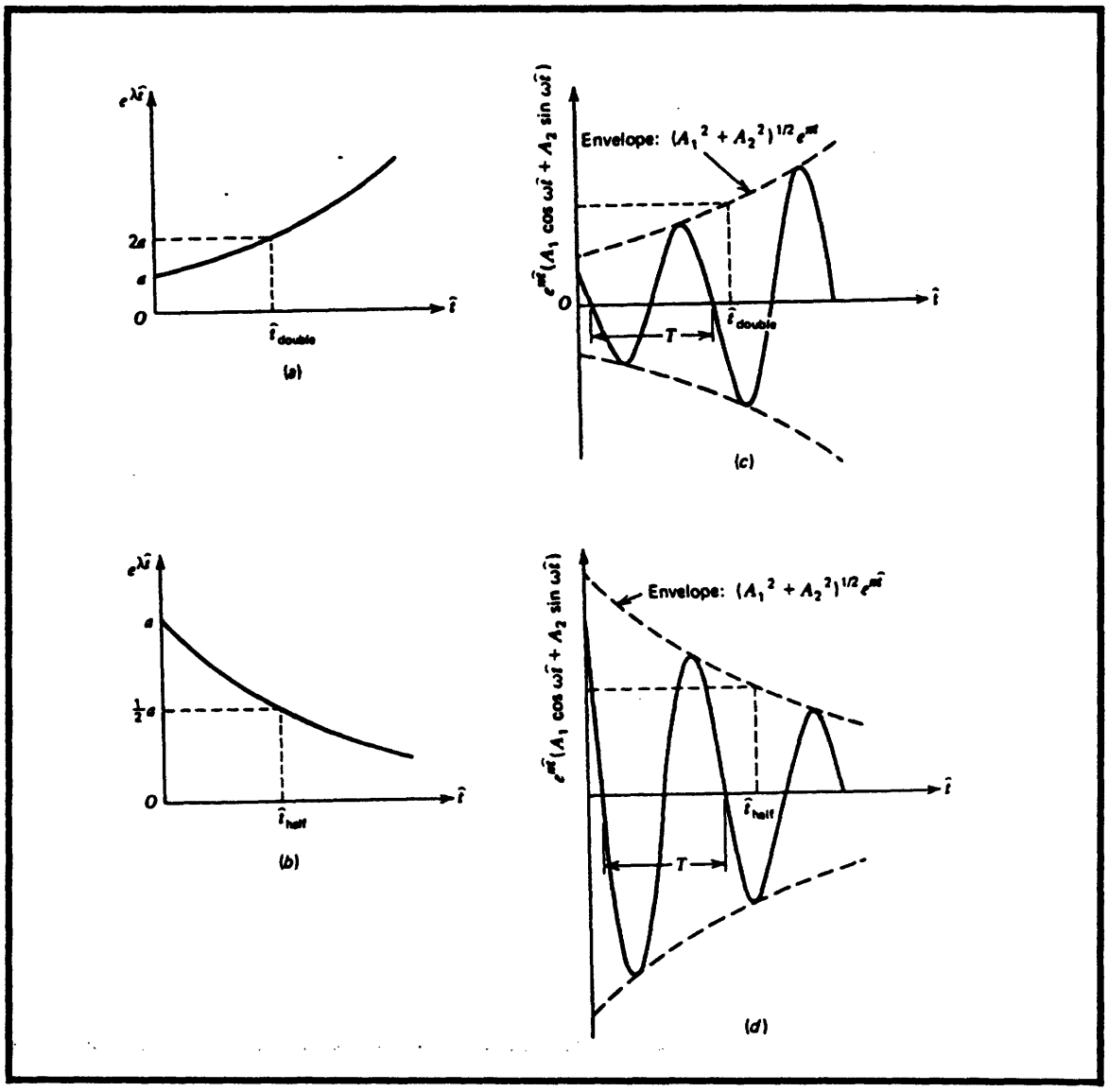

Figure 3.1 - Modes of Motion (a) Real-Positive (b) Real-Negative (c) Complex-Positive Real Part (d) Complex-Negative Real Part

The equations of motion describing aircraft dynamics have coefficients which vary as the aircraft flies along a prescribed trajectory. Under these conditions the system stability is not necessarily given by the location of the roots of the frozen approximation [10]. The system may have roots entirely in the left half plane and still be unstable, or it may have roots in the right half plane and be stable. Therefore, frozen approximations to root locations are not adequate to predict the stability of the system. As will be seen later, asymptotic approximations in closed analytical form will be developed from which the stability of the system can be predicted.

LONGITUDINAL MODES OF MOTION

The longitudinal perturbation equations of motion are

1. $(s - X_u)\Delta u - X_\alpha \Delta\alpha + g\Delta\theta = 0$
2. $-Z_u \Delta u + (s - Z_\alpha)\Delta\alpha - su\Delta\theta = 0$
3. $-M_v \Delta v - (M_{\dot\alpha} s + M_\alpha)\Delta\alpha + (s - M_{\dot\theta})s\Delta\theta = 0$

The equations are put in to the form $A\underline{x} = 0$ where $\underline{x}$ is the vector of perturbation variables and A is the matrix of coefficients. This form of the equations is called the state-space form and is useful in analyzing the solutions to the equations.

$$\begin{bmatrix} (s - X_u) & -X_\alpha & g \\ -Z_u & (s - Z_\alpha) & -su \\ -M_u & -(M_{\dot\alpha} s + M_\alpha) & (s - M_{\dot\theta})s \end{bmatrix} \begin{bmatrix} \Delta u \\ \Delta\alpha \\ \Delta\theta \end{bmatrix} = \begin{bmatrix} 0 \\ 0 \\ 0 \end{bmatrix}$$

The stability of each perturbation variable is determined by the characteristic equation (det/A/ = 0). The stability of each variable will be the same when there are constant coefficients in the A matrix. However, with variable coefficients, each variable may have different stability characteristics [10]. The longitudinal characteristic equation is a fourth order differential equation with variable coefficients.

$$s^4 + c_3 s^3 + c_2 s^2 + c_1 s + c_0 = 0$$

where

$$c_3 = -M_{\dot{\theta}} - Z_{\alpha} - X_u - uM_{\dot{\alpha}}$$

$$c_2 = -Z_{\alpha}M_{\dot{\theta}} - X_{\alpha}Z_u + -uM_{\alpha} + X_uM_{\dot{\theta}} + X_uZ_{\alpha} + X_uuM_{\dot{\alpha}}$$

$$c_1 = -X_u(Z_{\alpha}M_{\dot{\theta}} - uM_{\alpha}) + Z_u(X_{\alpha}M_{\dot{\theta}} + gM_{\dot{\alpha}}) - M_u(uX_{\alpha} - g)$$

$$c_0 = g(Z_{\alpha}M_{\alpha} - M_uZ_{\alpha})$$

The roots of the longitudinal characteristic equation define the modes of motion. The longitudinal equations normally have two modes corresponding to two pairs of complex conjugate roots. Figure 3.2 shows the typical root locations for the longitudinal mode [9].

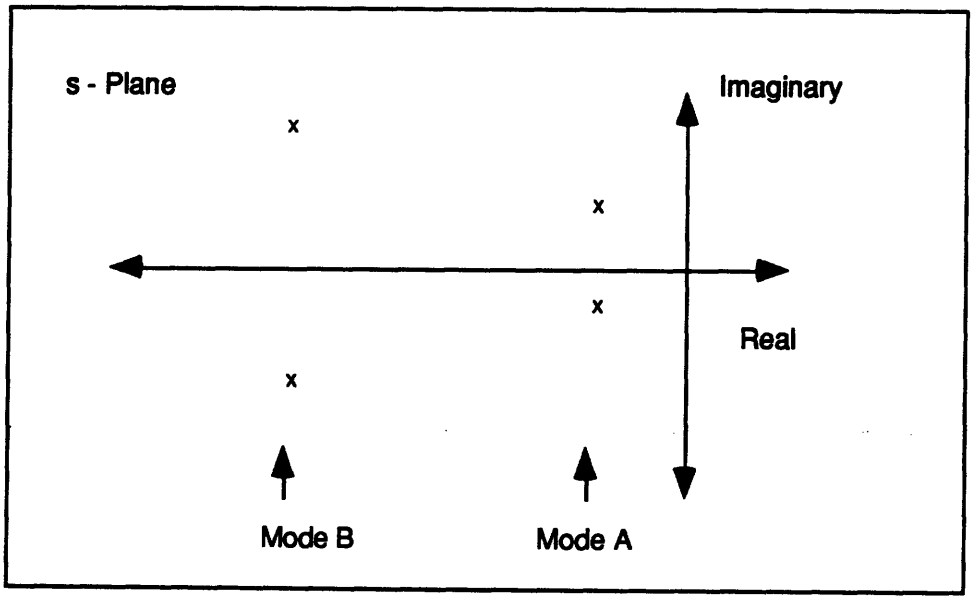

Figure 3.2 - Longitudinal Roots

A. Phugoid Mode - low frequency and low damping results in slowly damped oscillation.

B. Short Period Mode - high frequency and high damping results in quickly damped oscillation.

LATERAL-DIRECTIONAL MODES OF MOTION

The lateral-directional perturbation equations of motion are

1. $(s - Y_v)\Delta v + (u - Y_r)s\Delta\psi - (g\cos\phi_0)\Delta\phi = 0$
2. $-L_v\Delta v + (\frac{I_{xz}}{I_{xx}}s^2 - L_r s)\Delta\psi + (s^2 - L_p s)\Delta\phi = 0$
3. $N_v\Delta v + (s^2 - N_r s)\Delta\psi - (\frac{I_{xz}}{I_{zz}}s^2 - N_p s)\Delta\phi = 0$

These equations are expressed in state-space form and the modes of motion are determined from the characteristic equation.

$$\begin{bmatrix} (s - Y_v) & (u - Y_r) & -g\cos\phi_0 \\ -L_v & (\frac{I_{xz}}{I_{xx}}s^2 - L_r s) & (s^2 - L_p s) \\ -N_v & (s^2 - N_r s) & -(\frac{I_{xz}}{I_{zz}}s^2 + N_p s) \end{bmatrix} \begin{bmatrix} \Delta v \\ \Delta\Psi \\ \Delta\phi \end{bmatrix} = \begin{bmatrix} 0 \\ 0 \\ 0 \end{bmatrix}$$

The lateral-directional characteristic equation is also a fourth order differential equation with variable coefficients.

$$c_4 s^4 + c_3 s^3 + c_2 s^2 + c_1 s + c_0 = 0$$

where

$$c_4 = 1 - \frac{I_{xz}^2}{I_{xx}I_{zz}}$$

$$c_3 = -Y_v(1 - \frac{I_{xz}^2}{I_{xx}I_{zz}}) - L_p - N_r$$

$$c_2 = uN_v + L_p(Y_v + N_r) + N_p(\frac{I_{XZ}}{I_{XX}}Y_v - L_r) + Y_v(\frac{I_{XZ}}{I_{ZZ}}L_r + N_r) + u\frac{I_{XZ}}{I_{ZZ}}L_v$$

$$c_1 = -uN_vL_p + Y_v(N_pL_r - L_pN_r) + uN_pL_v - g\cos\phi(L_v + \frac{I_{XZ}}{I_{XX}}N_v)$$

$$c_0 = g\cos\phi(L_vN_r - L_vL_r)$$

The lateral-directional equations normally have three modes corresponding to two real roots and one pair of complex conjugates. The typical root locations are shown in figure 3.3 [9].

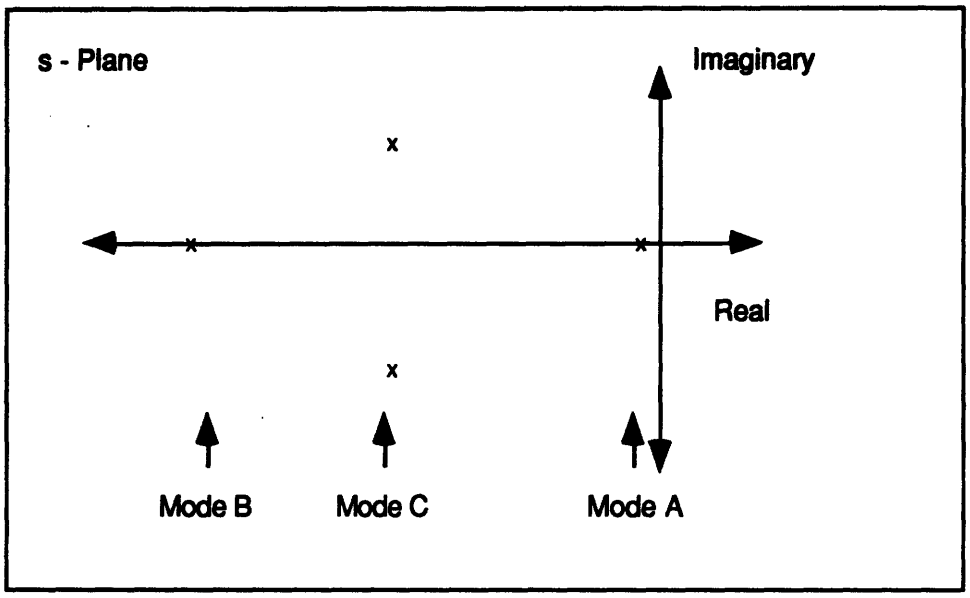

Figure 3.3 - Lateral-Directional Roots

A. Spiral Mode - Damped exponential response to yaw disturbance

B. Roll Mode - Damped exponential response to roll disturbance

C. Dutch Roll Mode - Damped oscillation of coupled roll-yaw motion

4. GHAME: HYPERSONIC AERODYNAMIC MODEL

INTRODUCTION

A Generic Hypersonic Aerodynamic Model Example (GHAME) was provided by NASA Ames Research Center for computer simulation [1]. The model consists of realistic data of aerodynamic coefficients in the hypersonic flight regime. The data was presented without analysis for the purpose of providing a simulation model for research and development analysis.

The model is based upon flight test data from the Space Shuttle and the X-24C and theoretical data from a swept double-delta configuration and a 6 degree half-angle cone using modified Newtonian Impact Flow method. The mission selected for the GHAME vehicle is a single-stage-to-orbit (SSTO). This entails taking off horizontally from a conventional runway, accelerating to orbital velocity as an air-breathing aircraft and insertion into a Low-Earth Orbit (LEO). After the mission is complete the aircraft would reenter the atmosphere and glide to a horizontal landing.

VEHICLE DESCRIPTION

The vehicle geometry was built from simple geometric shapes and is shown in figure 4.1 [1]. This allowed simplified estimates of the vehicle mass properties. The primary structure was modeled as a cylinder 20 feet in diameter and 120 feet long. This ensured the internal volume required for storage of the liquid hydrogen propellant. A pair of 10 degree half

angle cones were attached to this cylinder to form the nose and boat-tail and complete the fuselage assembly. The wings and vertical tail were modeled as thin triangular plates. The wings start at the fuselage midpoint

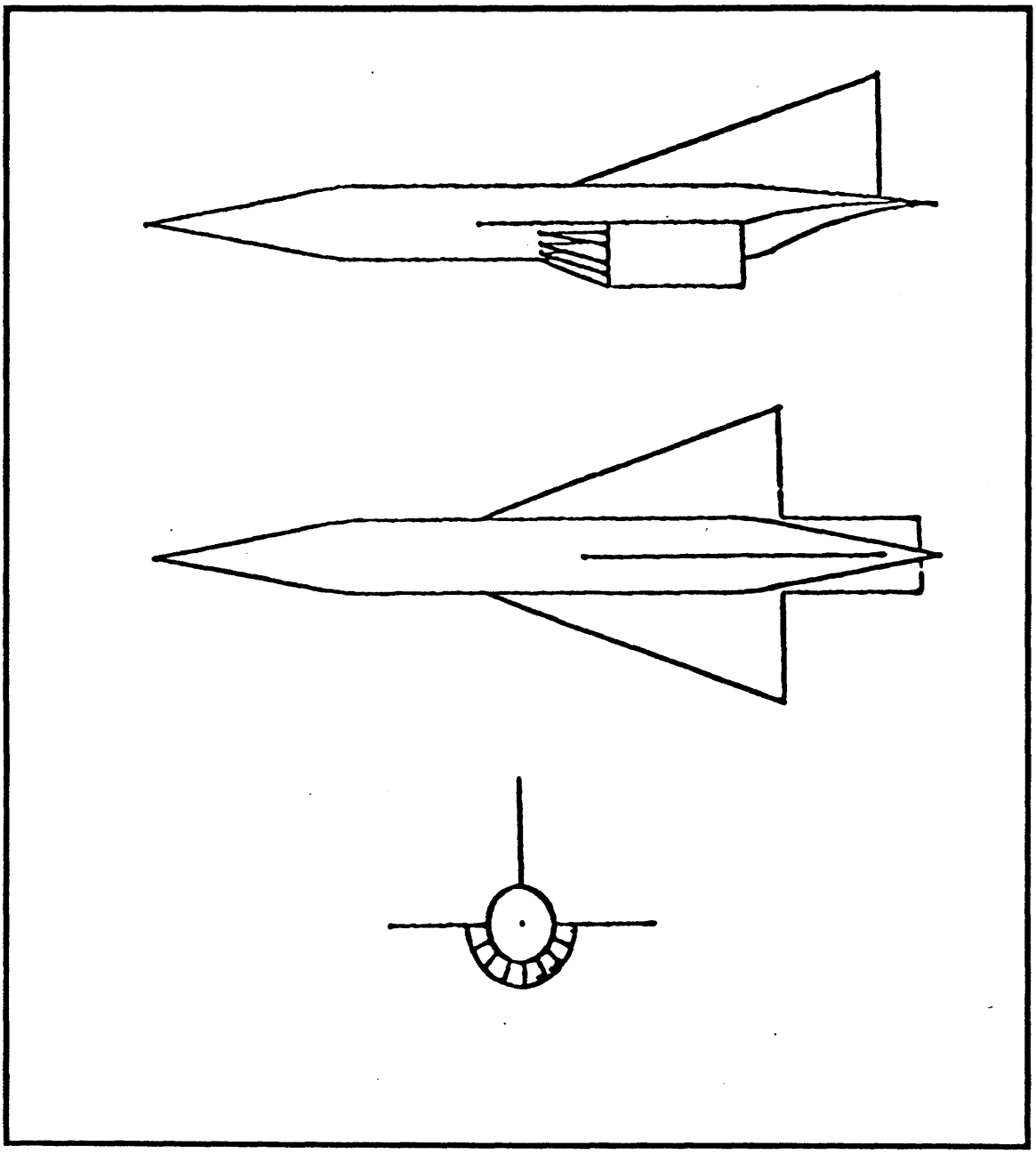

Figure 4.1 - GHAME Configuration

and have no dihedral angle. The engine module wraps around the lower surface of the fuselage. The overall length is 233.4 ft with the following aerodynamic design parameters: the reference area is 6,000 ft^2, the reference chord is 75 ft, and the reference span is 80 ft.

MASS PROPERTIES

The mass properties of the GHAME vehicle were assumed to be of the same order of magnitude as current supersonic cruise aircraft and were specifically derived from the XB-70 aircraft [1]. The take off gross weight was modeled to be 300,000 pounds with 60% (180,000 pounds) as liquid hydrogen fuel. The nominal reference center of mass occurs at .33 x c_{mac}. The mass moments of inertia were then calculated from the simple geometric shapes used for the vehicle configuration and are listed below.

At take off:

$I_{XX} = 1.16 \times 10^6$ slug-ft^2

$I_{YY} = 23.3 \times 10^6$ slug-ft^2

$I_{ZZ} = 24.0 \times 10^6$ slug-ft^2

$I_{XZ} = 0.28 \times 10^6$ slug-ft^2

At fuel burn out:

$I_{XX} = 0.87 \times 10^6$ slug-ft^2

$I_{YY} = 14.2 \times 10^6$ slug-ft^2

$I_{ZZ} = 14.9 \times 10^6$ slug-ft^2

$I_{XZ} = 0.28 \times 10^6$ slug-ft^2

AERODYNAMIC DATA

GHAME data consists of tables of aerodynamic coefficients used to calculate forces and moments on the aircraft for simulation purposes. Each coefficient varies as a function of Mach number and angle of attack. They are arranged in data arrays of 13 by 9 with row variation according to Mach number (0.4, 0.6, 0.8, 0.9, 0.95, 1.05, 1.2, 1.5, 2.0, 3.0, 6.0, 12.0, 24.0) and column variation according to angle of attack in degrees (-3.0, 0.0, 3.0, 6.0, 9.0, 12.0, 15.0, 18.0, 21.0). The symbolic notation used to describe the aerodynamic data is presented below.

Symbolic Notation of Aerodynamic Coefficients:

A. Superscripts

C_L - coefficient of lift force

C_D - coefficient of drag force

C_Y - coefficient of side force

C_M - coefficient of pitching moment

C_l - coefficient of rolling moment

C_n - coefficient of yawing moment

B. Subscripts

-0 zeroth coefficient term

-α alpha coefficient term (per degree)

-β beta coefficient term (per degree)

-P roll rate (radian per second)

-Q pitch rate (radian per second)

-R yaw rate (radian per second)

The GHAME data is used for simulation by providing aerodynamic data at discrete points along a trajectory according to Mach number and angle of attack. This data is used to calculate the forces and moments acting on the aircraft. This information defines the equations that govern its dynamic motion. The following chapters describe the simulation of the GHAME model along an entry trajectory and present a method to analyze the differential equations resulting from computer simulation.

5. DESCRIPTION OF ENTRY TRAJECTORY

INTRODUCTION

The trajectory used to study the GHAME vehicle dynamics was chosen to follow the entry trajectory flown by the Space Shuttle Orbiter [4]. This decision was made to provide a realistic trajectory currently being flown by an existing hypersonic vehicle (HSV). The entry guidance of the Space Shuttle Orbiter provides steering commands to control the entry trajectory from initial penetration of the Earth's atmosphere until activation of terminal area guidance. The unpowered entry guidance of HSVs is complicated because of physical flight constraints (temperature, g-load, dynamic pressure), termination requirements, variations in atmospheric density, uncertainties in vehicle mass and aerodynamic characteristics, measurement errors and time-varying control authorities. The trajectory is flown to minimize the demands on the vehicle systems and deliver the vehicle to a satisfactory attitude and energy state at activation of terminal area guidance.

GUIDANCE CONCEPT

The orbiter entry guidance is designed on the principle of defining a desired drag acceleration profile and commanding the vehicle attitudes to achieve the desired profile. The drag acceleration profile is based on vehicle system constraints and terminal attitude and energy state requirements. The systems of most concern are thermal protection system (TPS), flight control system (FCS) and vehicle structure.

The minimum weight and thickness required for the TPS is achieved by minimizing the heat load into the structure and limiting the allowable surface temperature. These constraints are met by flying at the maximum angle of attack allowable for crossrange requirements.

Demands on the FCS are limited by minimizing the attitude maneuvering required by the guidance algorithm. This is accomplished by limiting the angular acceleration and rate for both the bank angle and the pitch angle. FCS requirements also limit the allowable dynamic pressure so that aerodynamic control surface hinge movements are small.

The internal vehicle structure weight is minimized by limiting the aerodynamic loads during entry. Because the total aerodynamic force during entry is essentially perpendicular to the vehicle longitudinal axis, the load constraint is achieved by limiting the normal aerodynamic load factor.

The activation of the terminal area guidance requires that the vehicle has an angle of attack no greater than the value corresponding to maximum L/D. This is achieved by a pitch down maneuver designed to reduce the angle of attack from its maximum value required by the TPS to a value near maximum L/D at activation of terminal area guidance.

The desired entry profile is defined based on vehicle constraints and termination requirements. A control law is then developed to compute guidance commands to control the vehicle to this profile. The commanded L/D required to maintain the reference profile is achieved by a combination of bank angle modulation and angle of attack modulation. Bank angle modulation is the primary trajectory control parameter because the angle of attack is selected to minimize aerodynamic heating.

Bank angle magnitude controls total range, and the direction of the bank angle controls vehicle heading. Roll reversals are accomplished to maintain heading within a specified error deadband. Trajectory response to bank angle modulation is slow due to low angular acceleration and rate capabilities, requiring the angle of attack to be modulated on a short period basis to maintain the reference profile and minimize the transient effects of bank angle reversals. Tables 5.1-5.3 present the vehicle constraints along the trajectory, the interface conditions to begin entry guidance and the desired termination conditions respectively [4]. Figure 5.1 presents the nominal values of parameters along the entry trajectory [6].

VEHICLE CONSTRAINTS & INTERFACE CONDITIONS

Aerodynamic Load	3.0 g's
Dynamic Pressure	1800 (lbf/ft^2)
Bank Acceleration	1.7 (deg/sec^2)
Bank Rate	5.0 (deg/sec)
Pitch Acceleration	5.0 (deg/sec^2)
Pitch Rate	2.0 (deg/sec)
Thermal	$T_{skin} < 2300$ F $Q_{net}(T_{max}) < 0$

Table 5.1 - Summary of Vehicle Constraints

Altitude	400,000 (ft)
Inertial Velocity	25,744 (ft/sec)
Earth-Relative Velocity	24,193.7 (ft/sec)
Altitude Rate	-576.1 (ft/sec)
Longitude	0 (deg)
Latitude	0 (deg)
Heading w.r.t. True North	90 (deg) equatorial orbit

Table 5.2 - Entry Interface Conditions

Altitude	80,000 (ft)
Earth-Relative Velocity	2500 (ft/sec)
Angle of Attack	8.5 (deg)
Heading w.r.t. True North	90 (deg)
Longitude	67.728 (deg)
Latitude	0 (deg)

Table 5.3 - Desired Termination Conditions

NOMINAL VALUES OF TRAJECTORY PARAMETERS

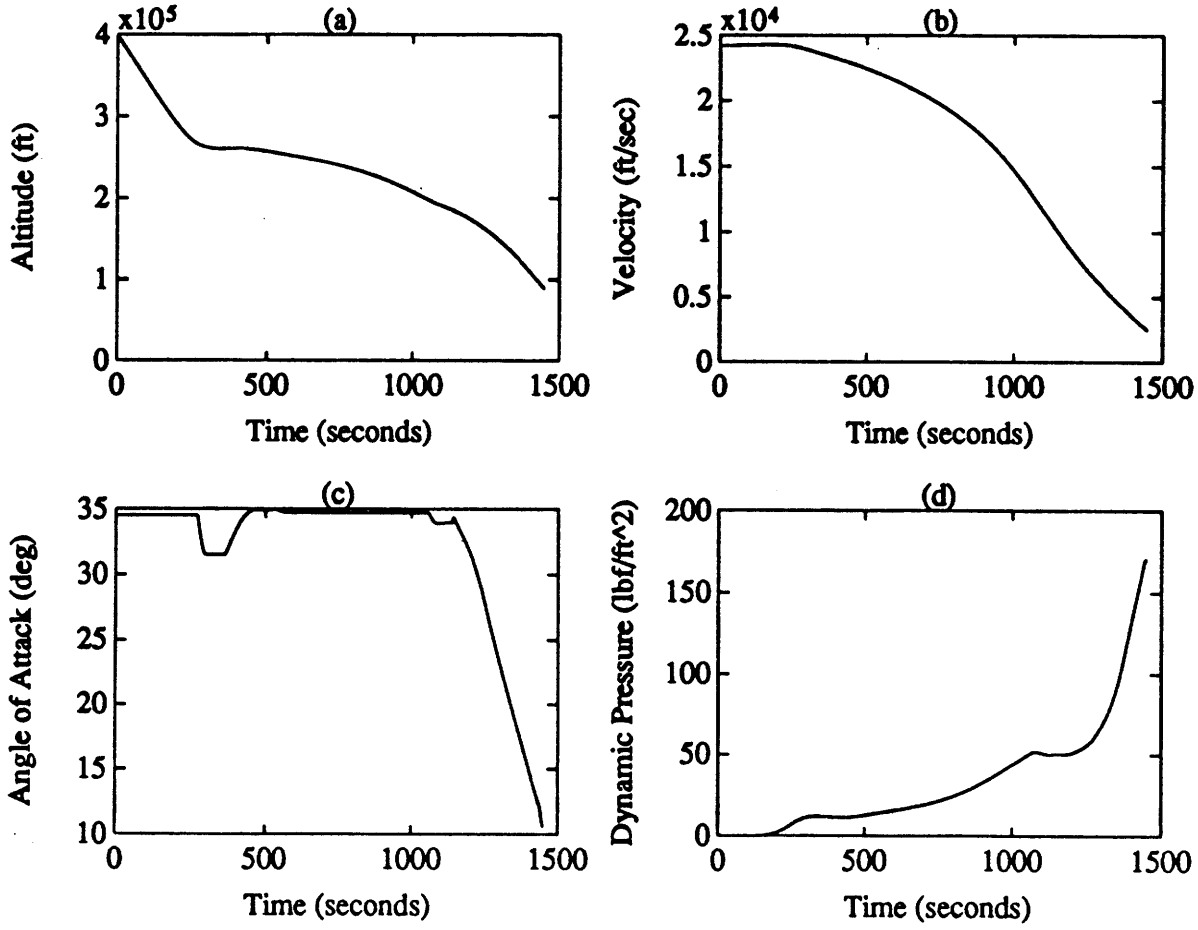

Figure 5.1 - Trajectory Parameters
(a) Altitude (b) Velocity
(c) Angle of Attack (d) Dynamic Pressure

6. GENERALIZED MULTIPLE SCALES TECHNIQUE

INTRODUCTION

Differential equations with varying coefficients, as seen in aircraft dynamics, cannot generally be solved exactly. For very particular variations of the coefficients, some equations can be solved in terms of special mathematical functions such as those of Bessel, Kummer or Mathieu. Even these solutions are only available as tabulated values. The technique of Generalized Multiple Scales developed by Ramnath [11-14] allows for the development of asymptotic approximate solutions to linear and nonlinear differential equations with time varying coefficients. These approximate solutions are in closed analytical form in terms of elementary functions such as sine, cosine and exponential and are uniformly valid over a wide range of the independent variable. The approximate solutions are possible by considering the dynamics of the system to occur much faster than the change in coefficients of the mathematical model. For aircraft dynamics problems the trajectory must be chosen so that the coefficients are slowly varying functions of the independent variable. The resulting asymptotic solutions turn out to be very good approximations to the actual solution and are very useful in the analysis of the system dynamics. This method has only been developed relatively recently, yet it is rapidly becoming well known.

DEVELOPMENT OF METHOD

The method of Generalized Multiple Scales (GMS) is used to develop asymptotic solutions to differential equations with time varying coefficients in terms of elementary functions. The method is general enough to include linear, nonlinear, ordinary and partial differential equations. This technique has its origins in the work on asymptotic analysis done by Poincare', Krylov and Bogoliubov who allowed the constants arising in direct perturbation theory to be slowly varying functions. Direct perturbation methods lead to nonuniformities in the solutions of many dynamic problems. This occurs because the solutions are expressed in an inappropriate scale. Physical systems often exhibit a mixture of rapid and slow dynamics, and separate scales are often necessary to describe their motion. An example of such a system is the motion of a satellite orbiting an oblate earth. The fast motion consists of an elliptical orbit while the slow motion consists of a rotation of the ellipse due to the oblateness. The GMS method eliminates the nonuniformities of direct perturbation theory by expressing the solution in multiple time scales. The fast and slow parts of the dynamics are separated through an extension of the independent variable. As a result of the extension, a system of ordinary differential equations is converted into one of partial differential equations. The system is then solved asymptotically, and the solutions are restricted to the original problem variables.

In order to achieve such a separation, the independent variable is extended into a space of higher dimension by means of nonlinear scale functions [10,14]. Instead of a one-to-one relationship between variables there is a one-to-many extension of the independent variable. This is a

generalization of the concept of variable transformations. The multiple scaling is not merely a transformation but an extension from one dimension to many dimensions. Each dimension is assumed to be independent, and the resulting equations are solved asymptotically [10,14].

As developed by Ramnath [10-14], the independent variable is extended into a higher dimension in terms of the small parameter ε in order to separate the fast and slow parts of the dynamics.

$$t \rightarrow \{\tau_0, \tau_1\}$$

$$\tau_0 = t \quad \text{(slow)}$$

$$\tau_1 = \frac{1}{\varepsilon}\int k(\xi)d\xi \quad \text{(fast)}$$

where $k(\xi)$ is a nonlinear scale function (or clock function), and τ_0 and τ_1 are treated as independent variables. The original problem variables become

$$x(t,\varepsilon) \rightarrow \overline{X}(\tau_0, \tau_1, \varepsilon)$$

The equation is ordered in terms of ε and solved asymptotically. The solution is then restricted to the problem variables of ε and t. This is not an exact solution, but it is a good approximation.

The scale function $k(\xi)$ can take on any value and is in general a complex quantity [10-14]. The small parameter ε which is introduced in order to apply the GMS technique falls out of the final form of the solution. It can be combined with the arbitrary constant of the approximation to yield a general form of the solution.

An essential aspect of using an approximation method is the error with respect to the function being approximated. The error at any stage of this asymptotic method is of the order of the first term neglected in the power series. The magnitude of each successive term in the expansion

decreases rapidly so a sufficiently accurate approximation can be obtained. In addition to this, Ramnath has shown that error theorems provide strict and sharp analytical bounds on the errors of approximation of the GMS method [14].

APPLICATION OF METHOD

The Generalized Multiple Scales technique has been applied by Ramnath and Sinha in their work " On the Dynamics of The Space Shuttle During Entry into Earth's Atmosphere" [14]. The method was used to develop an analytical asymptotic representation of the dynamics, in the plane of symmetry, of the Space Shuttle vehicle during entry into the earth's atmosphere. The procedure and results are presented here.

The angle of attack oscillations of a shuttle vehicle during entry into the atmosphere has been described by a unified equation developed by the work of Vinh and Laitone [15]. The result of their work is given by equation 6.1.

$$\alpha'' + \omega_1(\xi)\,\alpha' + \omega_0(\xi)\,\alpha = f(\xi) \qquad (6.1)$$

where the independent variable ξ is the distance traveled by the center of mass along the trajectory in terms of the number of reference lengths (L).

$$L\xi' = V(t)$$

The reference length represents the length of the vehicle being analyzed. The coefficients ω_1 and ω_0 are functions of aerodynamic parameters which vary with respect to the independent variable ξ [15]. They are determined from aerodynamic parameters by the following equations.

$$\omega_1(\xi) = \delta[C_{L\alpha} - s(C_{mq})] + (V'/V)$$

$$\omega_0(\xi) = -\delta(\sigma C_{m\alpha} + (gL/V^2)\, C_{D\alpha} \cos\gamma) + \delta' C_{L\alpha} + \delta(V'/V)\, C_{L\alpha}$$
$$-\delta^2[C_{L\alpha}(\sigma C_{mq} + C_{D0}) + C_{L0}\, C_{D\alpha}] + (3L/r)(gL/V^2)\, \upsilon \cos 2(\gamma+\alpha_0)$$

where

$$\delta = \rho S L/2m$$

$$\upsilon = (I_{xx} - I_{zz})/I_{yy}$$

$$\sigma = mL^2/I_{yy}$$

The primes denote differentiation with respect to ξ. The coefficients can be determined explicitly if the trajectory flown by the center of mass is known and the aerodynamic parameters can be determined.

It is, in general, impossible to integrate equation 6.1 exactly in order to obtain a solution. Previous work done by Vinh and Laitone show that for two specific entry trajectories equation 6.1 can be reduced to well-known dynamic equations. For a straight line ballistic entry at steep angles the equation is reduced to a Bessel equation of zeroth order [15]. For a shallow gliding entry the equation can be described as a damped Mathieu equation with periodic forcing terms [15]. These equations can be solved exactly but only from tabulated values and are applicable only when the trajectory is one of these specific cases. A typical entry trajectory will fall somewhere in between the steep straight line entry and the shallow gliding entry. A more general approach is needed to analyze the dynamics of vehicles traveling along a typical trajectory. These two specific forms of the equation provide an analytical feel for the system from which to develop general asymptotic solutions.

Experience with entry trajectories of missiles and the Space Shuttle show that the coefficients ω_1 and ω_0 are slowly varying along the trajectory. From penetration of the earth's atmosphere at about 400,000 feet until

terminal guidance is activated at about 80,000 feet, the variation in the coefficients are primarily due to changes in density, velocity, and the aerodynamic force and moment parameters along the the entry trajectory. These variations are slow compared to the time constant of the vehicle dynamics. Therefore the coefficients of equation 6.1 can be shown to vary according to a slow variable $\xi = \varepsilon\xi$, where ε is a small positive parameter which is a measure of the ratio of the time constant of the vehicle dynamics to the variation in the coefficients. The asymptotic solution is developed as this separation becomes greater or as ε goes to zero.

The small parameter ε is introduced into equation 6.1 in order to apply the GMS technique. Equation 6.1 is parameterized in terms of ε and written as

$$\varepsilon^2\alpha'' + \varepsilon\omega_1(\xi)\alpha' + \omega_0(\xi)\alpha = f(\xi)$$

The fast and slow parts of the dynamics are separated by an extension of the independent variable through scale functions. For oscillatory dynamics the scale function $k(\xi)$ is necessarily a complex quantity. The real and imaginary parts are denoted by

$$k(\xi) = k_r(\xi) + ik_i(\xi)$$

From this separation, analytical approximate solutions can be obtained through the GMS method.

The solution to the unified angle of attack equation developed by Vinh and Laitone using the GMS technique was developed by the work of Ramnath and Sinha [14]. The resulting solution is presented here.

$$\alpha(\xi) = \alpha_s(\xi)\,\alpha_f(\xi)$$

where $\alpha_s(\xi)$ is the slow part of the solution and $\alpha_f(\xi)$is the fast part. The fast part is described by

$$\alpha_f(\xi) = C_1\left[\exp\left(\int k_r(\xi)d\xi\right)\sin\left(\int k_i(\xi)d\xi\right)\right] + C_2\left[\exp\left(\int k_r(\xi)d\xi\right)\cos\left(\int k_i(\xi)d\xi\right)\right]$$

or

$$\alpha_f(\xi) = C_1\alpha_{f_{sin}}(\xi) + C_2\alpha_{f_{cos}}(\xi)$$

where C_1 and C_2 are arbitrary constants which incorporate the small parameter ε. The fast scale solution primarily describes the frequency and phase of the solution. The slow part of the solution is described by

$$\alpha_s(\xi) = (\omega_1^2 - 4\omega_0)^{-1/4}$$

and primarily contributes to the amplitude of the oscillations. The resulting asymptotic solution to equation 6.1 determined by the GMS method with both fast and slow dynamics is

$$\alpha(\xi) = (\omega_1^2 - 4\omega_0)^{-1/4}\left[C_1\alpha_{f_{sin}}(\xi) + C_2\alpha_{f_{cos}}(\xi)\right]$$

The Generalized Multiple Scales solution to the unified angle of attack equation were applied by Ramnath and Sinha to study the dynamics of the the Space Shuttle [14]. The shuttle is flown along a typical entry trajectory and the variation of the coefficients of the governing equation (6.1) are tracked. The independent variable is defined as the nondimensional distance along the trajectory (ξ). The coefficients are seen to be slowly varying functions of the independent variable.

A reference solution to equation 6.1 is determined through numerical integration while allowing the coefficients to vary along the trajectory. A "frozen" approximate solution is determined by holding the coefficients constant at their initial values. These solutions are compared to those obtained from the analytical asymptotic solutions derived from the GMS method. The results show that the "frozen" approximation is not an adequate representation of the dynamics. It fails to predict the dynamics

of the system beyond the first quarter cycle of the oscillation. The fast part of the GMS solution predicts the frequency variations well, but has a small error in amplitude. This is corrected by including the slow part of the solution. The result shows that the GMS approximation to the first order represents the true solution very well [14]. This technique will be applied in the following chapters to the equations describing the GHAME vehicle dynamics along an entry trajectory.

7. GHAME SIMULATION AND MODES OF MOTION

SIMULATION

In this chapter the coefficients of the equations describing the dynamics of the GHAME vehicle will be recorded along an entry trajectory. Ramnath's GMS technique will be applied to these equations in the following chapter. The unified angle of attack equation developed by Vinh and Laitone will be used to describe the angle of attack oscillations of the GHAME vehicle. The coefficients of this equation as well as those describing the longitudinal and lateral-directional dynamics of the GHAME vehicle will be recorded. A complete Fortran implementation of the current shuttle entry guidance algorithm was applied. The code was adapted for MACINTOSH simulation of the GHAME vehicle model [6]. The simulation of the vehicle dynamics is based on a table look-up method. At each discrete point along the trajectory the stability derivatives are obtained from data tables according to Mach number and angle of attack. A linear extrapolation routine is used to determine the stability derivatives when the flight condition exceeds the limits of the tabulated values [6]. A weighted average routine determines the stability derivatives when the flight condition falls between the tabulated values [6].

The entry guidance simulation begins at an altitude of 400,000 feet with the appropriate velocity, position and attitude as described in Chapter Five. It continues for fourteen hundred and fifty seconds until termination of the entry guidance algorithm. The independent variable along the trajectory is changed, as was done by Vinh and Laitone, in order to apply

the GMS technique presented in the previous chapter. The independent variable ξ is the distance traveled by the center of mass along the trajectory in terms of the number of reference lengths (L).

$$L\xi' = V(t)$$

The reference length used in this simulation was 150 feet to represent the length of the GHAME vehicle. The value of the independent variable ξ is recorded at discrete points along the trajectory. It is a nonlinear function of time and has a range from zero to 1.68066×10^5.

The stability derivatives for the GHAME vehicle are calculated along the entry trajectory and presented in Figures 7.1 and 7.2. Figure 7.1 presents the longitudinal stability derivatives while Figure 7.2 presents the lateral-directional derivatives. The independent variable ξ is labeled "ksi".

The stability derivatives are used to calculate the coefficients of the unified angle of attack equation for the GHAME vehicle as well as the coefficients of the longitudinal and lateral-directional characteristic equations. These equations are integrated using a fourth order Runge-Kutta integration routine. Their coefficients are recorded at discrete points along the trajectory, and the roots of each are determined using the software application MatLab. The root locations are plotted in the complex plane as they vary along the trajectory in the following sections.

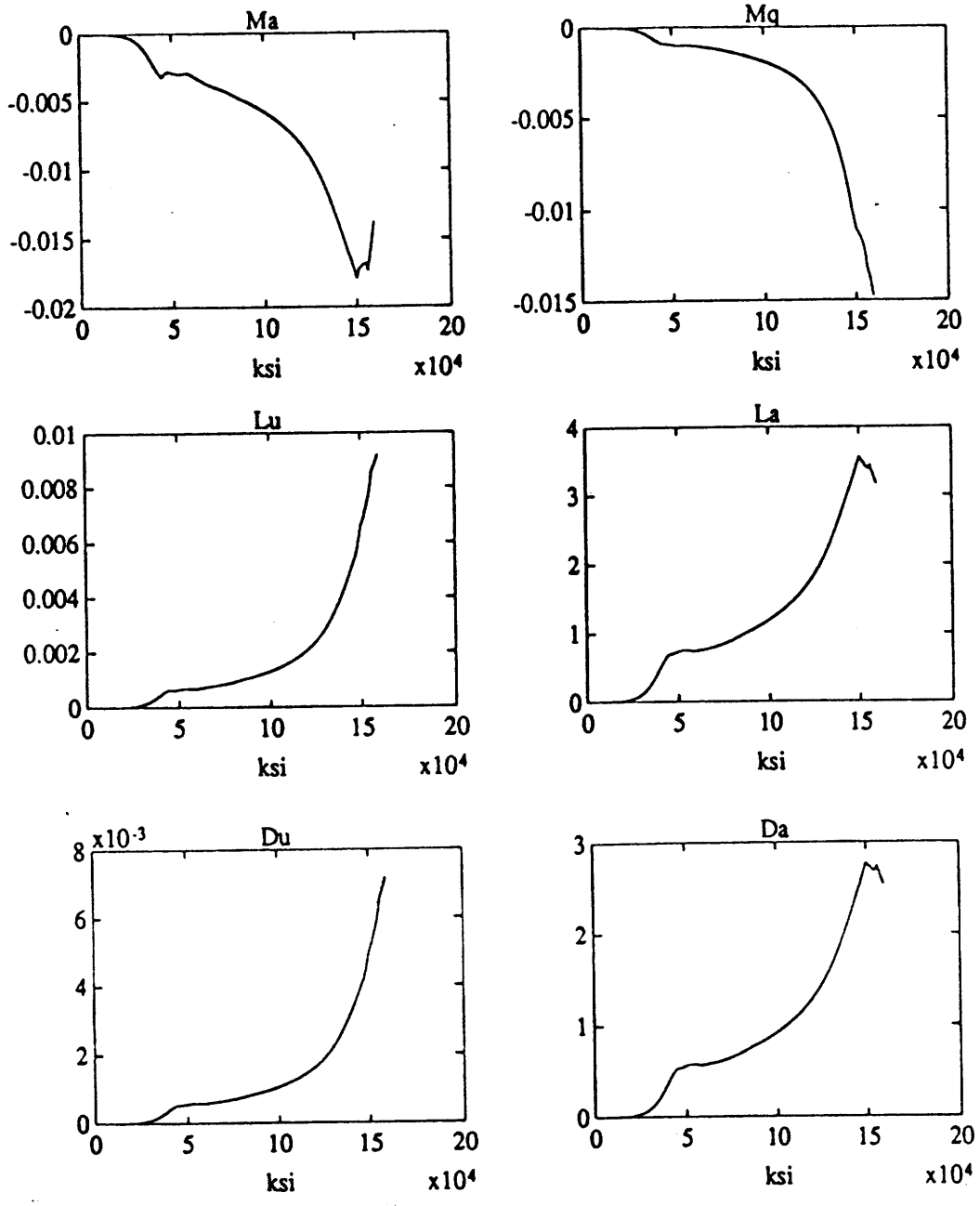

Figure 7.1 Longitudinal Stability Derivatives

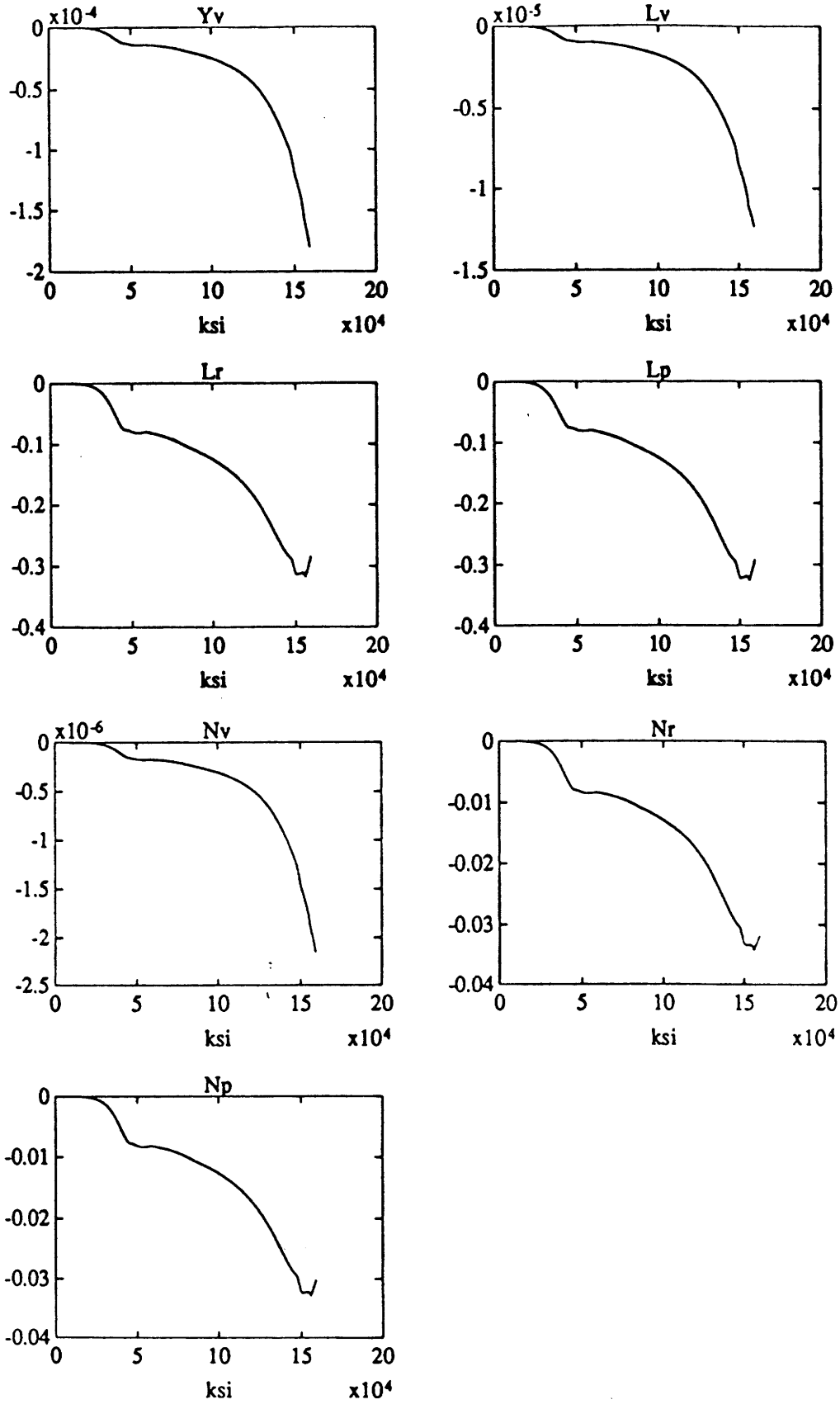

Figure 7.2 Lateral-Directional Stability Derivatives

UNIFIED ANGLE OF ATTACK DYNAMICS

The angle of attack dynamics of the GHAME vehicle are described by the unified equation developed by Vinh and Laitone as shown in the previous chapter. The coefficients of this equation are recorded as the vehicle flies along the entry trajectory. They are presented in Figure 7.3.

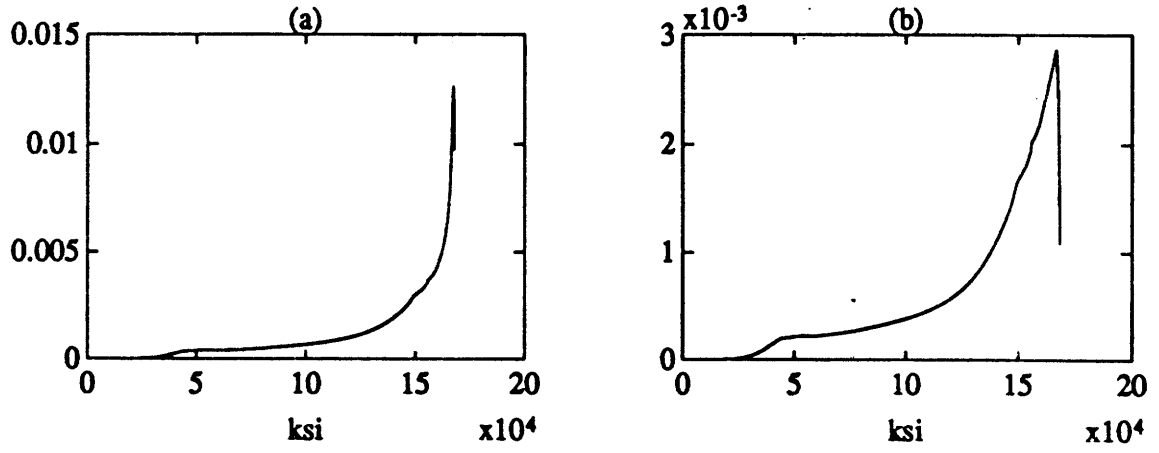

Figure 7.3 Coefficients of Unified Angle of Attack Equation (a) ω_1 (b) ω_0

Both quantities, ω_1 and ω_0, are slowly increasing functions with the independent variable. At the end of the trajectory they both experience a sharp downward spike. The sudden change in direction occurs at the same time as the downward pitching maneuver initiated by the guidance algorithm. This can be seen in the angle of attack profile for this trajectory shown in Chapter Five. The solutions to be developed by the GMS technique require that the coefficients be slowly varying quantities. The sharp spike might lead to complications resulting from a turning point in the solution. At a turning point there is a transition from one type of solution to another such as a transition from an oscillatory solution to an

exponential solution. The transition occurs in the vicinity of the turning point. Therefore, the trajectory will be restricted to eliminate this problem. The independent variable ξ will will be restricted to a range from zero to 1.6×10^5.

The roots of the unified angle of attack equation are plotted in the complex plane in Figures 7.4 and 7.5. Figure 7.4 presents the roots over the restricted trajectory; ξ [0, 1.6×10^5]. Figure 7.5 presents an expanded view of the roots at the origin in order to have a better view of how they begin. The roots begin at "x" and end at "o". The results show one pair of

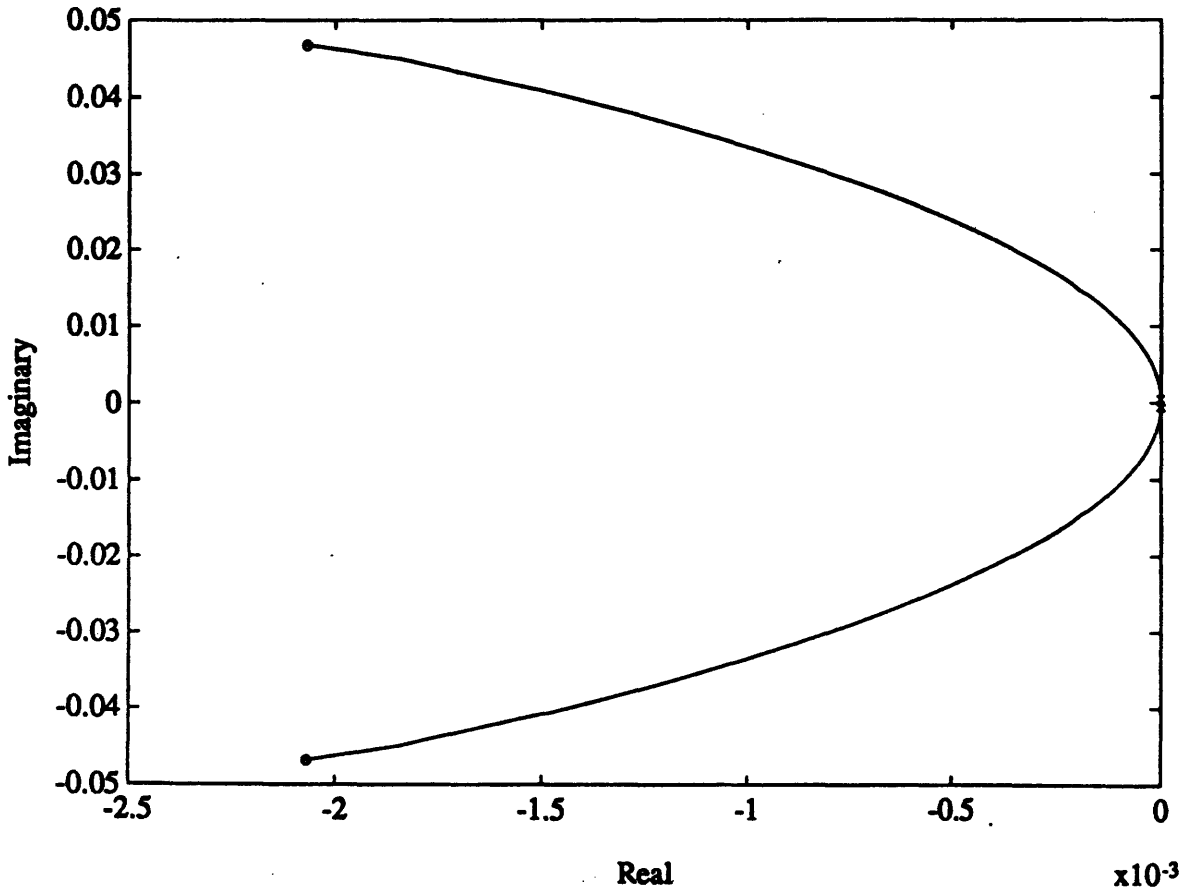

Figure 7.4 Unified Angle of Attack Roots Along Entry Trajectory

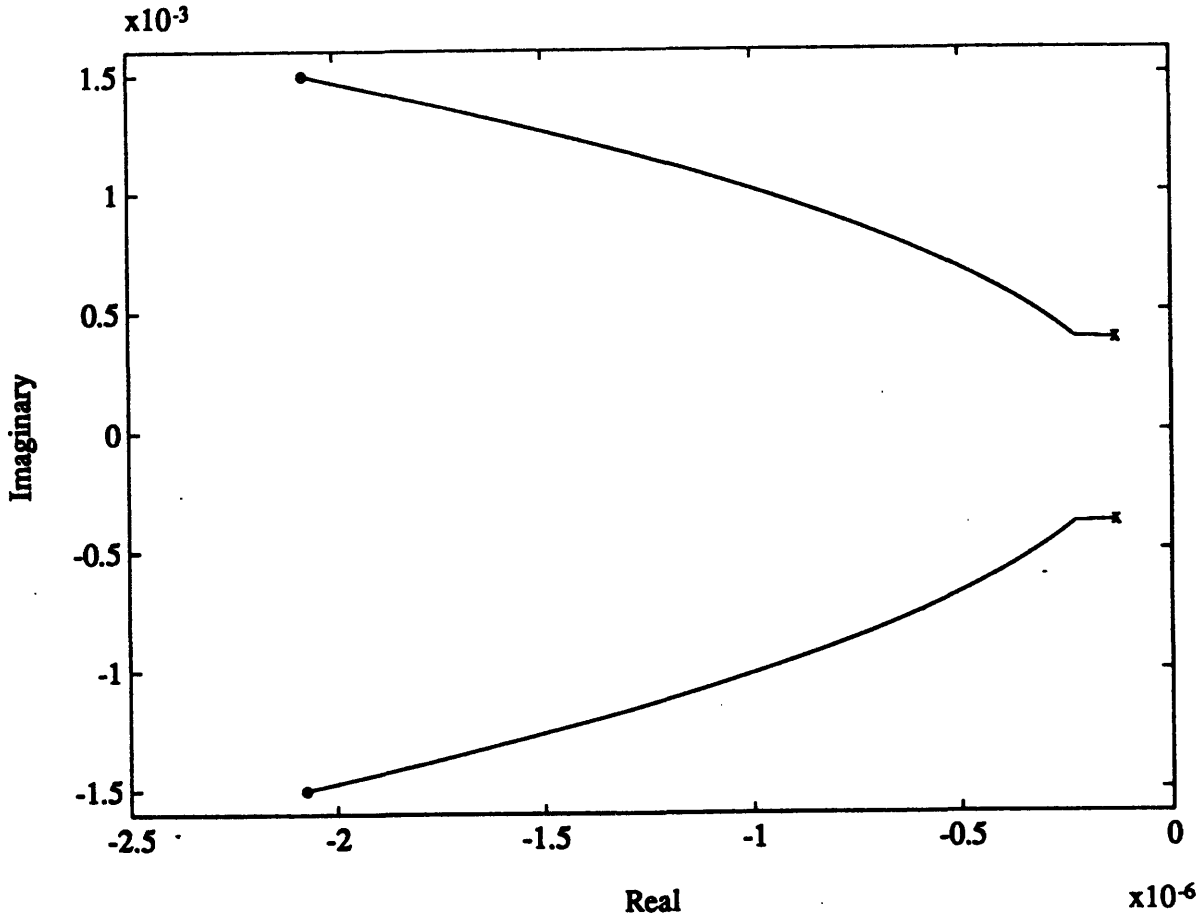

Figure 7.5 Expanded View of Unified Angle of Attack Roots

complex conjugate roots. These will be used in the following section as the scale functions of the GMS solutions. The expended view shows that they begin near the origin inside the left half plane and move farther into the left half plane along the trajectory. They increase in both frequency and damping as they move. Constant coefficient theory suggests that this is a stable mode with roots entirely in the left half plane. The solution will be some sort of damped oscillation.

LONGITUDINAL MODES OF MOTION

The longitudinal perturbation equations were simplified for the GHAME simulation by determining the following derivatives to be zero for this vehicle.

$$M_u \qquad M_{\dot{\alpha}}$$

The angle of attack is taken to be constant at 34 degrees. This is an adequate approximation because the angle of attack does not vary much over the course of the trajectory. The pitch down maneuver occurs at the end of the trajectory and is neglected for this simulation. The roots of the

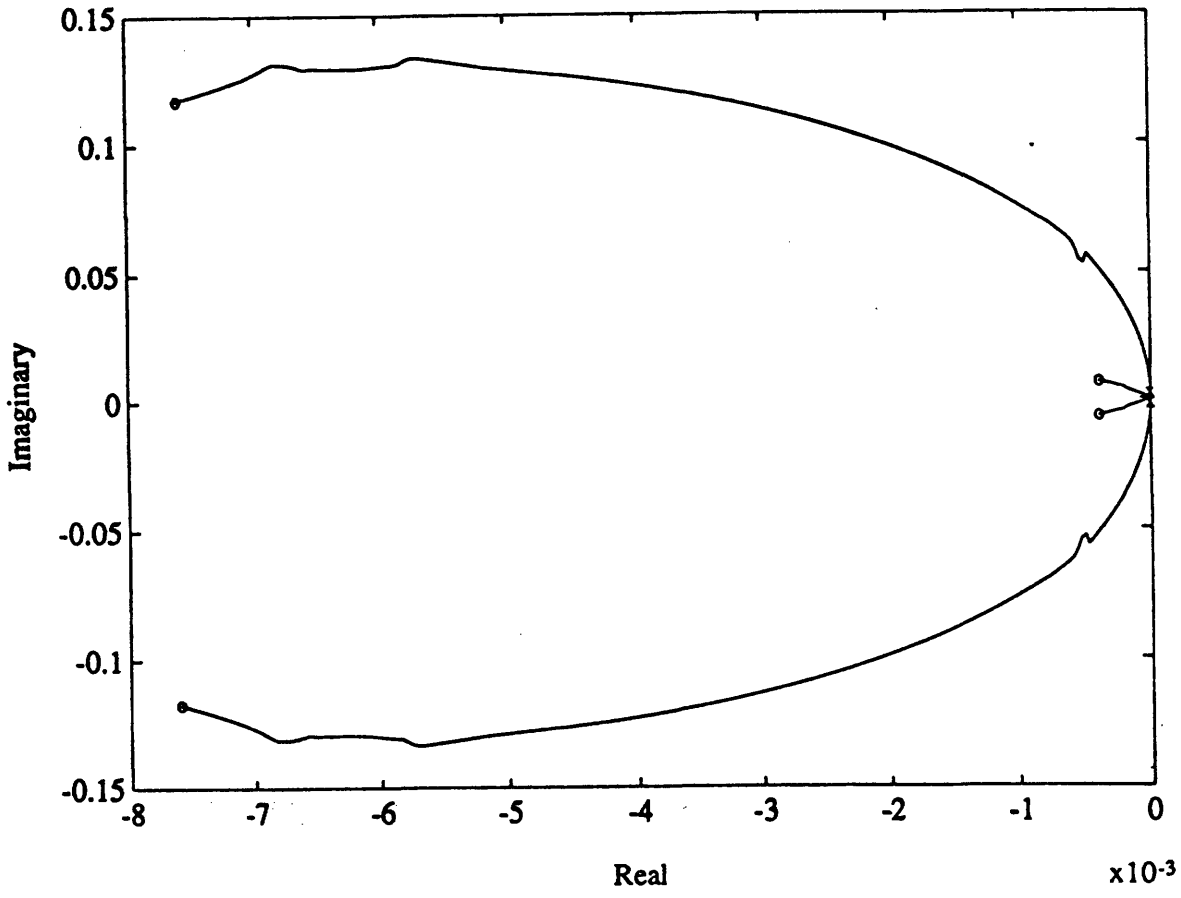

Figure 7.6 Longitudinal Roots Along Entry Trajectory

longitudinal characteristic equation vary along the trajectory and are plotted in the complex plane in Figures 7.6 and 7.7. The roots begin at "x" and end at "o". Figure 7.6 presents the roots over the restricted trajectory, ξ [0,1.6x10^5], while Figure 7.7 shows the roots in an expanded view at the origin.

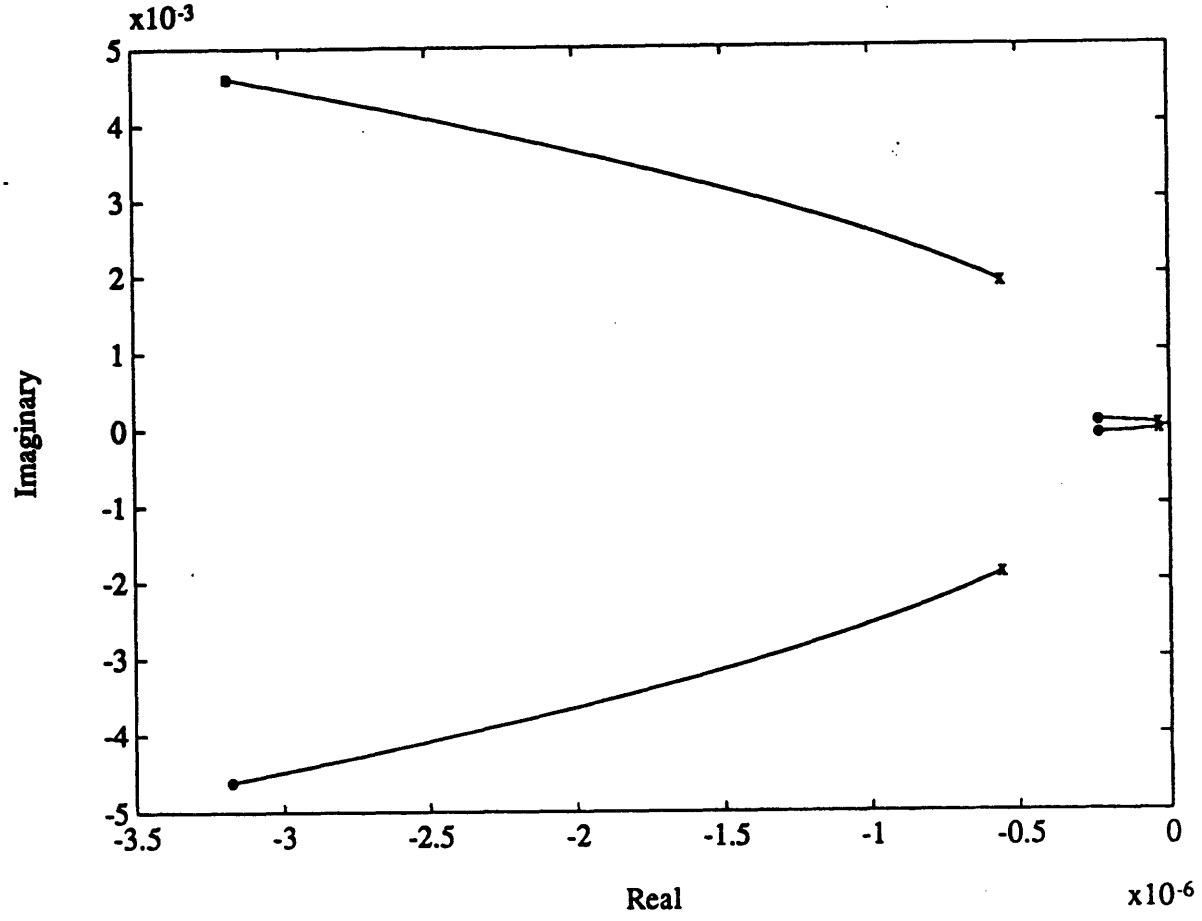

Figure 7.7 Expanded View of Longitudinal Roots

The results show a typical pattern of two pairs of complex conjugate roots describing the longitudinal motion of the GHAME vehicle. These will be used for the scale functions of the GMS solutions. Mode A (near the origin) corresponds to the Phugoid mode described in Chapter Three. Mode

B (far from the origin) corresponds to the Short Period mode. As seen in the expanded view, both pairs of roots begin near the origin of the complex plane. They begin inside the left half plane and move further into the left half plane as the GHAME vehicle travels along the trajectory. Both pairs show an increase in frequency and damping as they move. The Phugoid roots show a very small movement from the origin while the Short Period roots experience a large increase in both frequency and damping. The expanded view of the roots at the origin in Figure 7.7 reveals that they are always in the left half plane. Constant coefficient theory again suggests that these are both stable modes based on the root locations.

LATERAL-DIRECTIONAL MODES OF MOTION

The lateral-directional perturbation equations of motion were simplified by determining that Y_r equals zero for this vehicle and the quantity I_{xz}^2/I_{xx} is small enough to be considered zero. The root locations of the GHAME vehicle's lateral-directional modes are shown in Figures 7.8 and 7.9. Figure 7.8 shows the roots over the restricted trajectory while Figure 7.9 shows the roots in an expanded view at the origin.

The results show three distinct modes corresponding to those described in Chapter Three. There is one real root in the right half plane corresponding to the Spiral mode, one real root in the left half plane corresponding to the Roll mode and one complex pair corresponding to the Dutch Roll mode. According to constant coefficient theory the root locations show that the Spiral mode is unstable, the Roll mode is stable and the Dutch Roll mode begins unstable and moves to a region of stability.

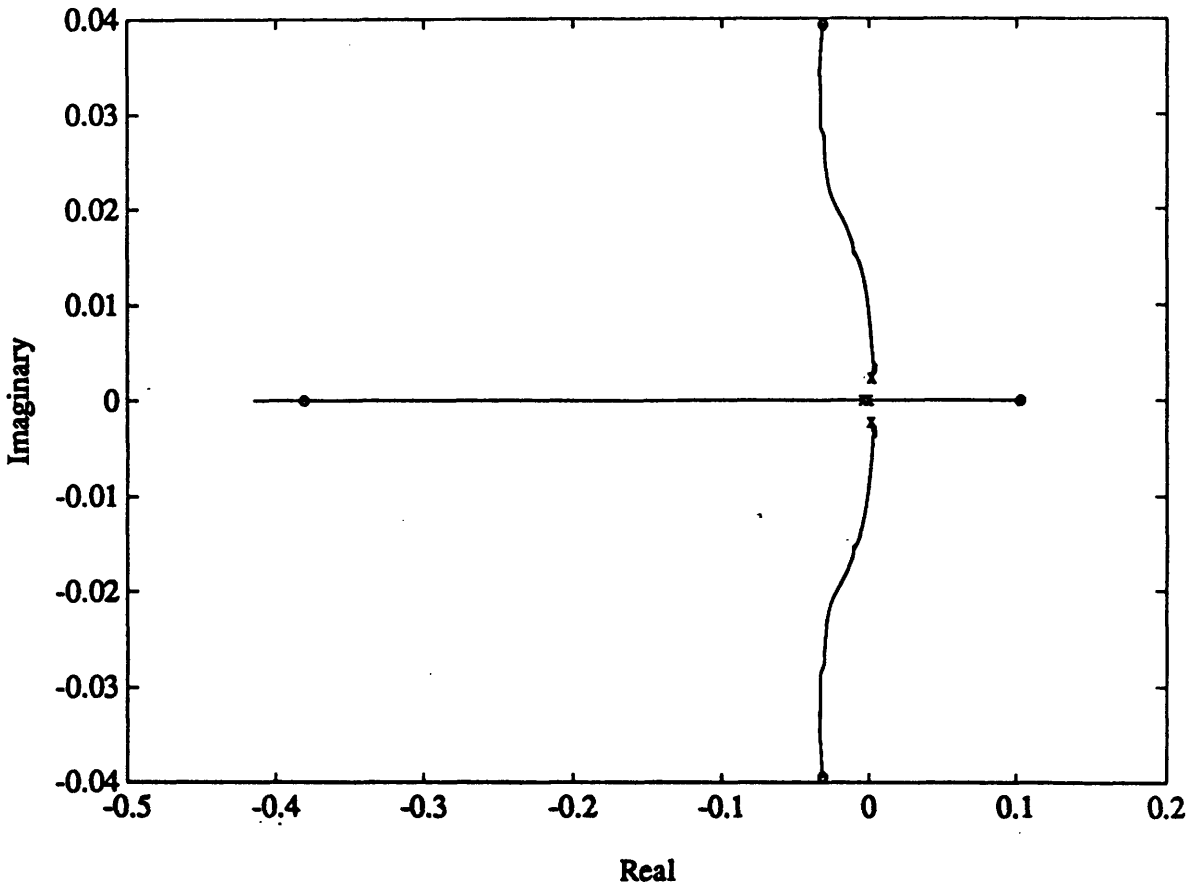

Figure 7.8 Lateral-Directional Roots Along Entry Trajectory

The expanded view shows that all the roots begin near the origin. The Spiral mode moves along the real axis into the right half plane while the Roll mode moves along the real axis into the left half plane. The complex Dutch Roll mode begins in the right half plane and initially moves further into that plane. It then reverses direction and begins to move toward the left half plane. The Dutch Roll mode primarily increases in frequency with only a slight increase in damping and ends up in the left half plane. This movement would indicate that the solution is initially an unstable oscillation and then becomes a stable oscillation.

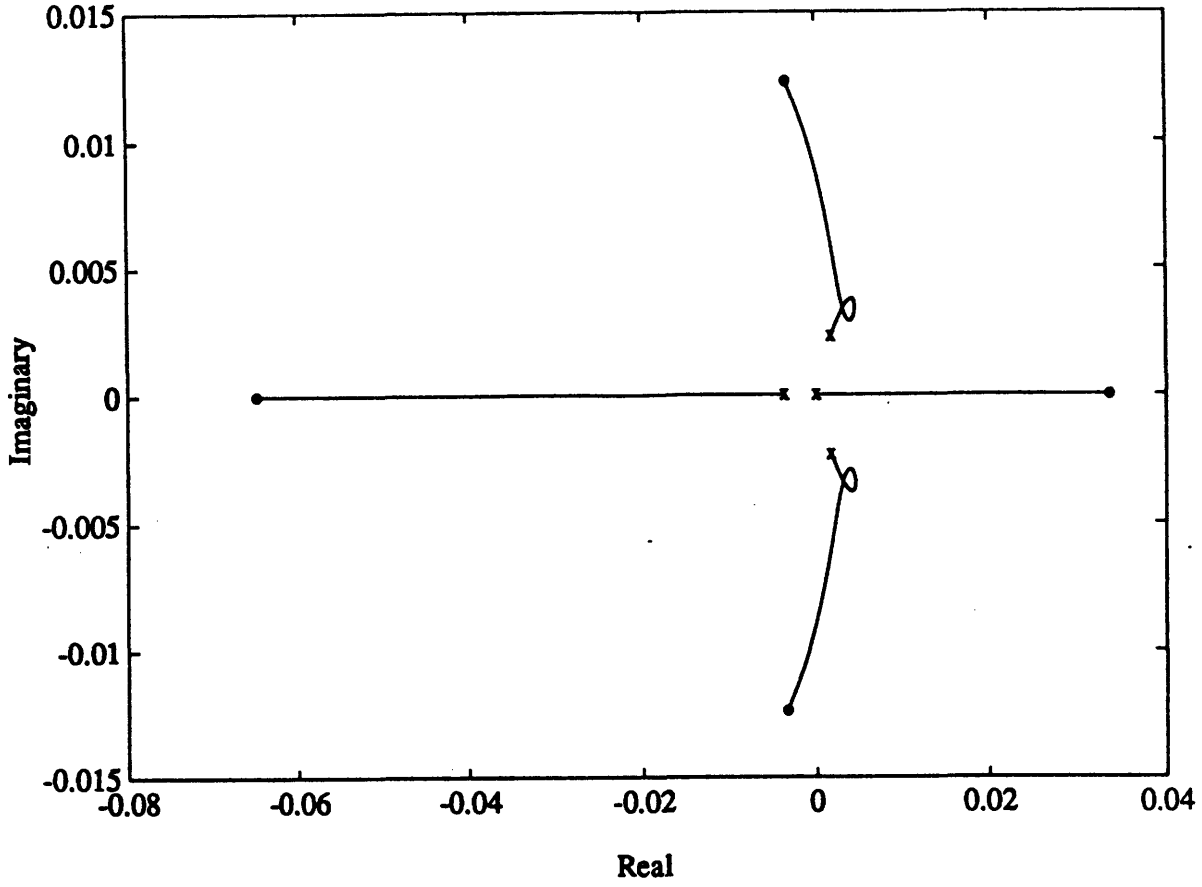

Figure 7.9 Expanded View of Lateral-Directional Roots

Root locations of constant coefficient differential equations are sufficient to determine the stability of their dynamics. However, root locations are not sufficient to completely predict the stability of systems with variable coefficients such as those which describe the GHAME dynamics. These systems can exhibit counter intuitive behavior with respect to their root locations [10]. A system with variable coefficients may have roots entirely in the left half plane and yet be unstable, while a system may have roots in the right half plane and be stable. Therefore, the GMS technique is applied to these equations to obtain analytical approximate solutions. From these solutions stability characteristics can be determined and control laws can be formulated.

8. SOLUTIONS TO GHAME EQUATIONS OF MOTION

UNIFIED ANGLE OF ATTACK DYNAMICS

The Generalized Multiple Scales (GMS) technique will be applied in this chapter to develop approximate analytical solutions to the equations describing the dynamics of the GHAME vehicle. Reference solutions to the dynamics will be obtained through numerical integration and will be compared to the GMS solutions.

As seen in the previous chapter, the unified angle of attack dynamics of the GHAME vehicle is described as a second order differential equation and characterized by one oscillatory mode. This equation is numerically integrated using a fourth order Runge-Kutta routine to obtain a reference solution. The small parameter ε is introduced into the equation in order to make use of the GMS technique. The second order equation is parameterized by the following method

$$\ddot{X} + \frac{\omega_1 \dot{X}}{\varepsilon} + \frac{\omega_0 X}{\varepsilon^2} = 0$$

The coefficients, ω_1 and ω_0, are slowly varying quantities along the trajectory. The small parameter ε was determined to be 1/161 for this problem. An intuitive feel for arriving at the value of ε will be discussed later in this chapter. The numerical integration satisfies the initial conditions

$$X(0) = 0$$

$$\dot{X}(0) = 1$$

Before the GMS technique is applied, a "frozen" approximation of the solution is compared to the numerical solution. This is done by freezing the coefficients at their initial values and integrating as a constant coefficient differential equation. The numerical solution is compared to the "frozen" approximation in Figure 8.1. The independent variable ξ is labeled "ksi".

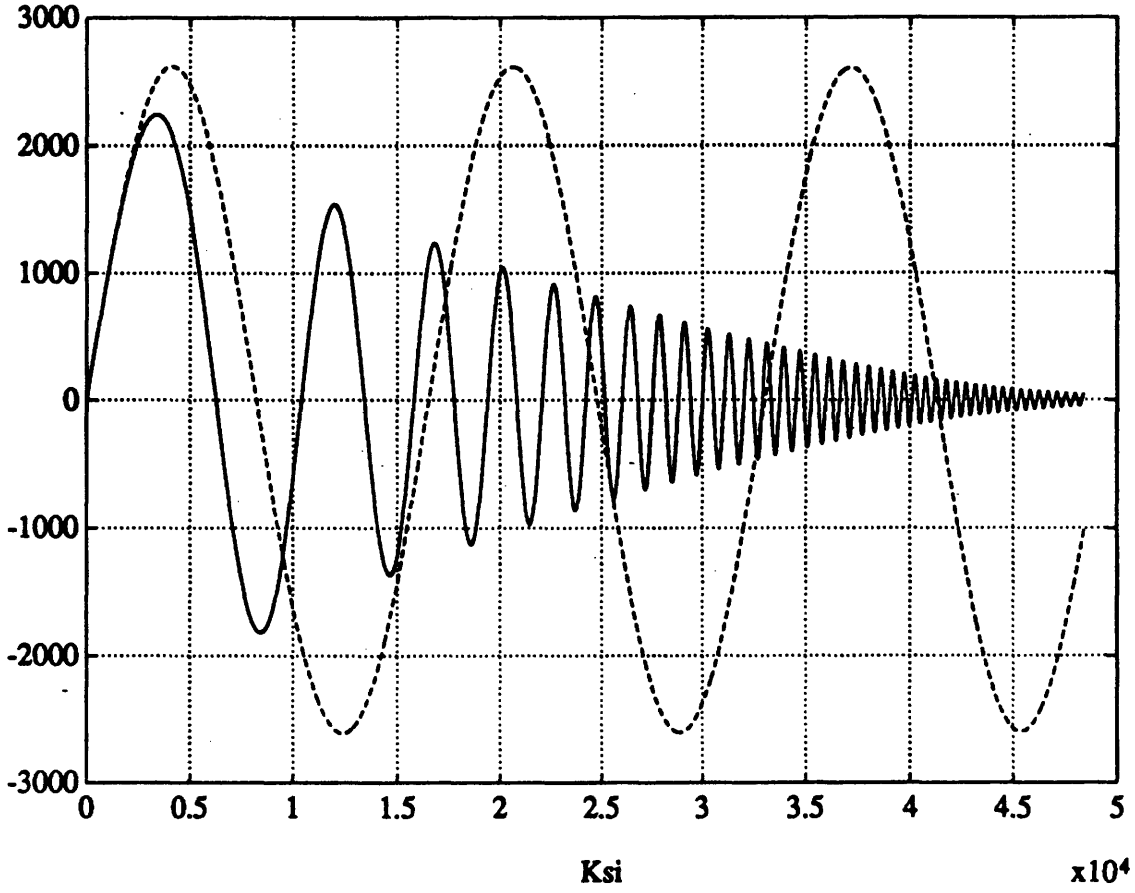

Figure 8.1 Numerical Solutions to Unified Angle of Attack Dynamics
solid - Numerical Solution
dashed - "Frozen" Approximation

The numerical solution shows a damped oscillation which increases in both frequency and damping along the trajectory. The results show that

the "frozen" approximation is not able to predict the dynamics beyond the first quarter cycle of the oscillation. This is clearly an inadequate representation of the vehicle motion and is not practical for applications involving stability and control analysis. Therefore, Ramnath's GMS technique will be used to develop a more accurate and practical approximation to the dynamics of the GHAME vehicle motion.

The GMS technique is applied to the GHAME equations of motion in order to determine analytical asymptotic approximations to the vehicle dynamics. The GMS solution to a second order differential equation with time varying coefficients was presented in Chapter Six to be

$$X(\xi) = X_s(\xi)X_f(\xi)$$

or

$$X(\xi) = (\omega_1^2 - 4\omega_0)^{-1/4}\left[C_1 X_{f_{sin}}(\xi) + C_2 X_{f_{cos}}(\xi)\right]$$

or

$$X(\xi) = (\omega_1^2 - 4\omega_0)^{-1/4}\left(C_1\left[\exp\left(\int k_r(\xi)d\xi\right)\sin\left(\int k_i(\xi)d\xi\right)\right] + C_2\left[\exp\left(\int k_r(\xi)d\xi\right)\cos\left(\int k_i(\xi)d\xi\right)\right]\right)$$

where C_1 and C_2 are determined by the initial conditions [14]. K_r is the real component of the complex root and k_i is the imaginary component.

This asymptotic analytical solution will be applied to the unified angle of attack equation and compared to the numerical solution. The GMS solutions must satisfy the same initial conditions as the numerical solution in order to compare the two. The constants C_1 and C_2 are determined in order to satisfy the initial conditions

$$X(0) = 0$$

$$\dot{X}(0) = 1$$

First, just the fast scale solution is considered.

$$X_f(0) = C_1 e^0 \sin(0) + C_2 e^0 \cos(0) = 0$$

$$C_2 = 0$$

$$\dot{X}_f(0) = C_1[k_r e^0 \sin(0) + k_i e^0 \cos(0)] + C_2[k_r e^0 \cos(0) - k_i e^0 \sin(0)] = 1$$

$$C_1 k_i + C_2 k_r = 1$$

$$C_1 = 1/k_i$$

The constants C_1 and C_2 are now derived for the complete GMS solution with both fast and slow response.

$$D^{-1/4} = (\omega_1^2 - 4\omega_0)^{-1/4}$$

$$X(0) = D^{-1/4}(C_1 \sin(0) + C_2 \cos(0)) = 0$$

$$C_2 = 0$$

$$\dot{X}(0) = D^{-1/4}(C_1 k_i + C_2 k_r) = 1$$

$$C_1 = 1/k_i D^{-1/4}$$

The GMS fast scale solution and the GMS combined solution are compared to the numerical solution for the angle of attack dynamics in Figure 8.2. The GMS fast scale solution accurately predicts the frequency of oscillation but over estimates the magnitude of the numerical solution. The slow scale correction adjusts the magnitude at the appropriate time and in the appropriate direction so that the combined GMS solution accurately predicts the angle of attack dynamics of the GHAME vehicle.

The GMS technique of approximating solutions to differential equations is dependent upon introducing a small parameter ε into the equation. The parameter ε must be much less than 1 to allow for the use of asymptotic analysis. The parameter ε is a measure of the ratio of the time constant of the vehicle dynamics to the time constant of the variation in the coefficients. Its value is determined in a trial and error fashion. The numerical solution is seen to increase in frequency as ε decreases. A

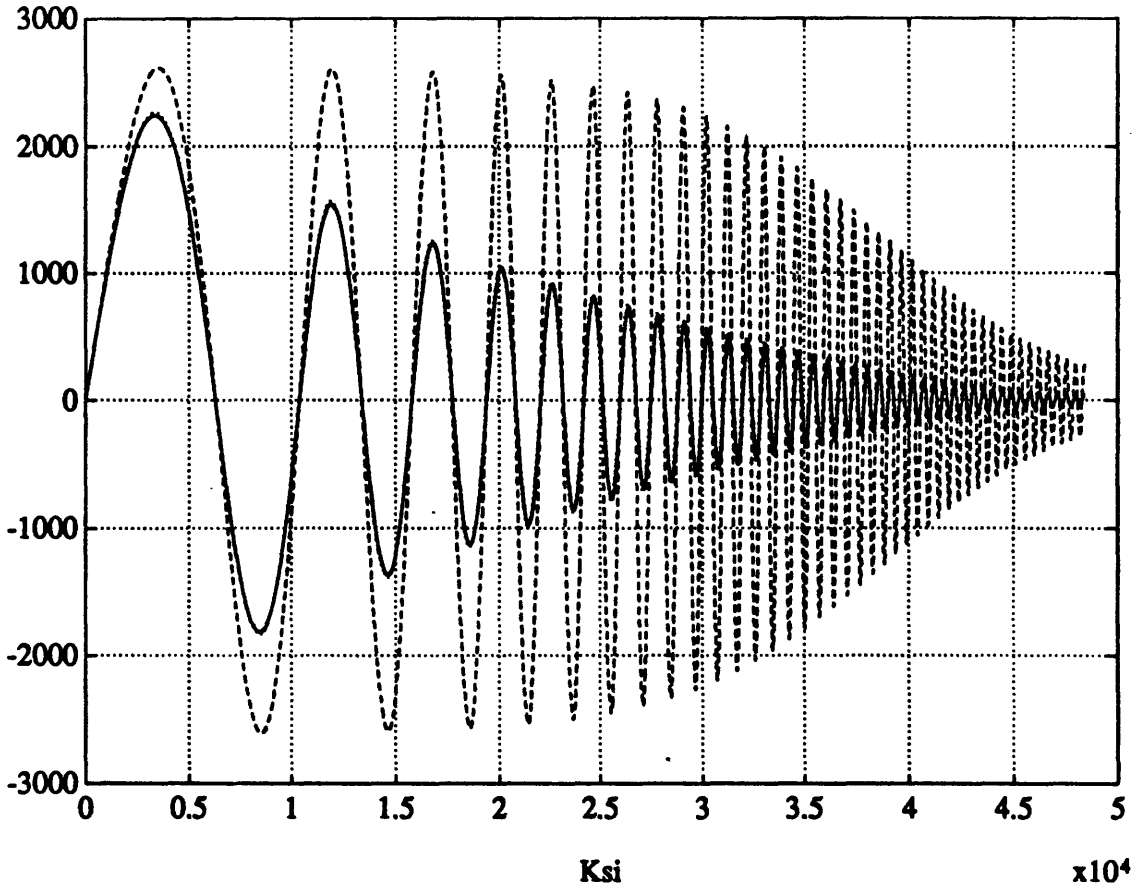

Figure 8.2 GMS Solutions to Unified Angle of Attack Dynamics
solid - Numerical Solution
dashed - GMS Fast Scale Solution
dotted - GMS Fast and Slow Scale Solution

proper value of ε leads to a match of the zero crossings of the numerical solution and those of the GMS solutions. The value of ε was determined to be 1/161 for the GHAME vehicle along the entry trajectory.

LONGITUDINAL DYNAMICS

The GMS technique will now be applied to the longitudinal motion of the GHAME vehicle. It was shown in the previous chapter that this motion is characterized by two oscillatory modes. The longitudinal motion can be conveniently represented by two second order differential equations, one equation for each mode. The reference solution to each mode of longitudinal motion is determined by numerical integration and compared to the "frozen" approximation. The GMS solution for each mode is then determined. It will be shown that the GMS solutions closely approximate the numerical solutions and can therefore be used for stability and control analysis.

A second order differential equation is constructed for each mode of the GHAME vehicle's longitudinal motion using the following technique.

$$\ddot{X}_A + \omega_1 \dot{X}_A + \omega_0 X_A = 0$$

$$\omega_1 = -(k_A + k_A^*)$$

$$\omega_0 = k_A(k_A^*)$$

where k_A and k_A^* are the roots corresponding to Mode A, and k_A^* is the complex conjugate of k_A. Similarly, a second order model for Mode B using k_B and k_B^* is constructed. The coefficients, ω_1 and ω_0, are slowly varying quantities along the trajectory for both modes.

The equations describing each mode are parameterized in terms of ε as was done in the analysis of the unified angle of attack dynamics (ε=1/161). The numerical solution for Mode A is compared to the "frozen" approximation in Figure 8.3. The numerical solution shows a damped oscillation which increases in both frequency and damping along the trajectory. This mode is characteristic of Phugoid motion. It has relatively

low frequency and low damping as might be expected from the root locations shown in the previous chapter to be near the origin. Again, the "frozen" approximation is unable to predict the dynamics of this mode beyond the first quarter cycle of the oscillation.

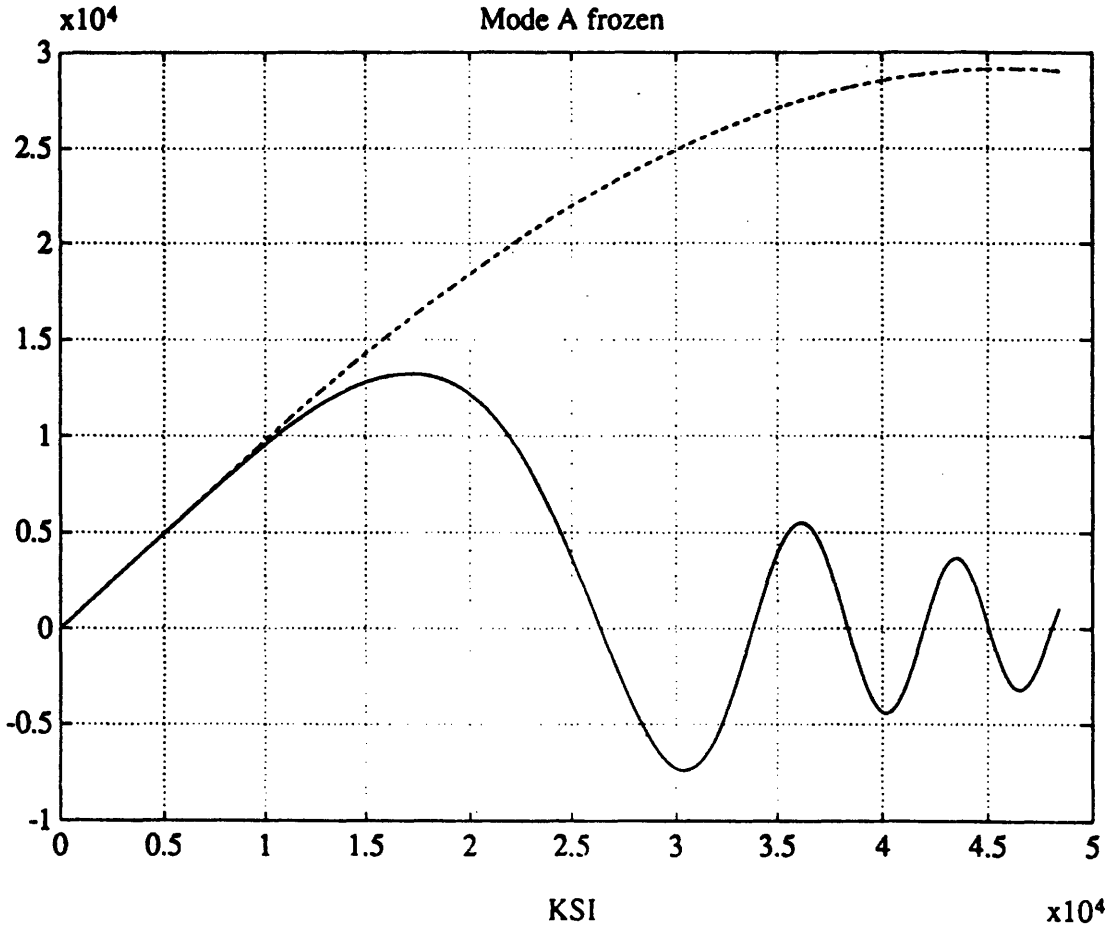

Figure 8.3 Numerical Solutions to Mode A
solid - Numerical Solution
dashed - "Frozen" Approximation

Figure 8.4 shows the numerical solutions for Mode B. The numerical solution is a damped oscillation which increases in both frequency and damping along the trajectory. This mode is characteristic of Short Period motion. It has relatively high frequency and high damping as might be

expected by its root locations shown to be far from the origin. The "frozen" approximation is unable to predict the actual dynamics beyond the first quarter cycle of the oscillation. Both "frozen" approximations for the longitudinal modes cannot predict the dynamics of the GHAME vehicle. They are inadequate for any practical application involving stability and control analysis.

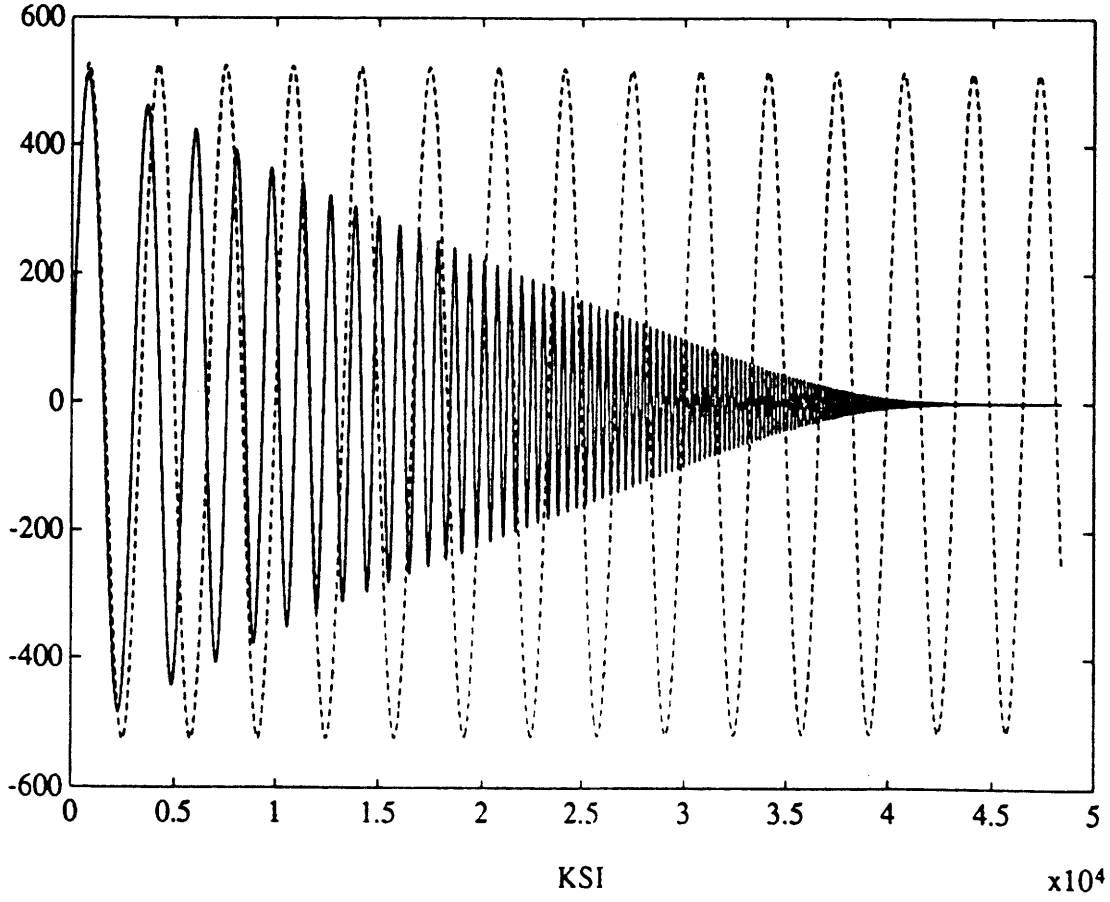

Figure 8.4 Numerical Solutions to Mode B
solid - Numerical Solution
dashed - "Frozen" Approximation

The GMS solutions are determined for each mode of longitudinal motion in the same way as was done for the unified angle of attack equation. They are compared to the reference solutions determined by numerical integration. The solutions to Mode A are shown in Figure 8.5. The GMS fast scale solution accurately predicts the frequency of oscillation but is shown to overshoot the magnitude of the numerical solution. The combined GMS solution accurately predicts the complete dynamics of the longitudinal motion of Mode A.

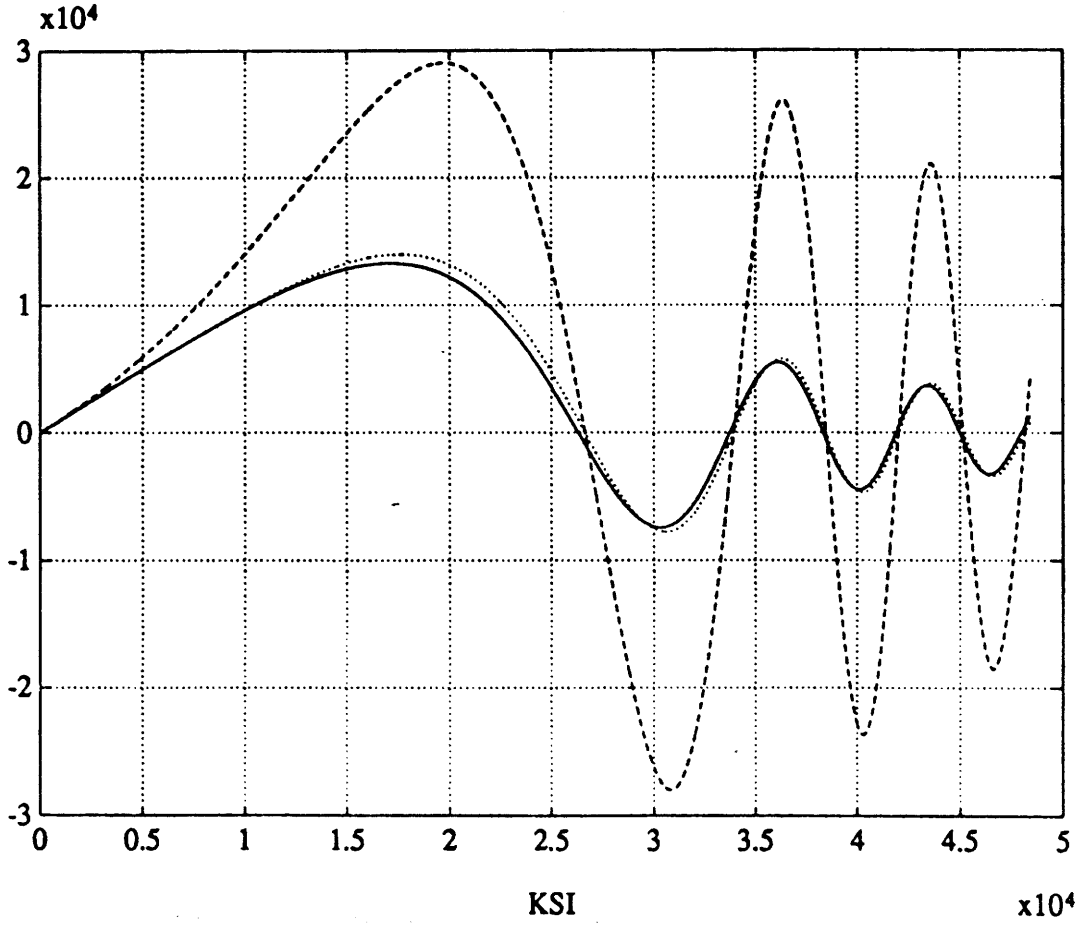

Figure 8.5 GMS Solutions to Mode A
solid - Numerical Solution
dashed - GMS Fast Scale Solution
dotted - GMS Fast and Slow Scale Solution

The same technique is applied to Mode B, and the solutions are shown in Figure 8.6. The results are similar. The GMS fast scale solution overshoots the numerical solution while the addition of the slow correction accurately predicts the dynamics of the longitudinal motion of Mode B.

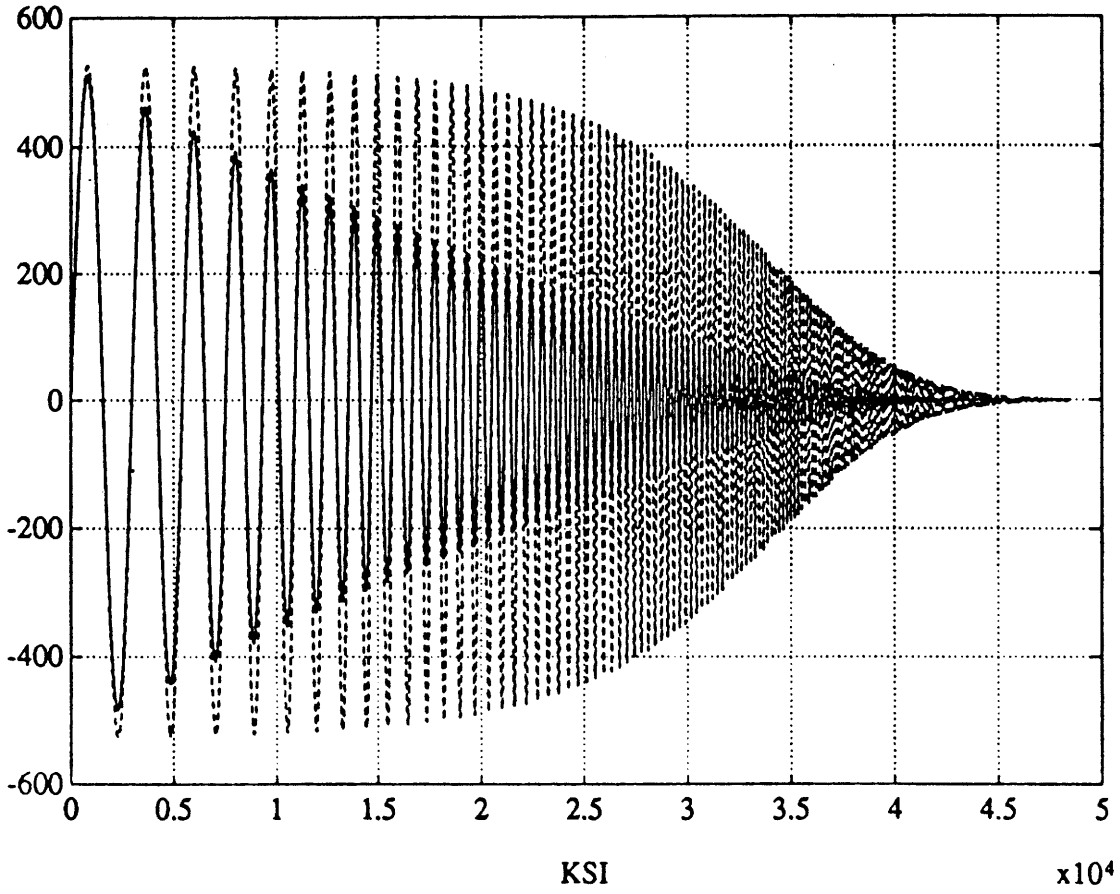

Figure 8.6 GMS Solutions to Mode B
solid - Numerical Solution
dashed - GMS Fast Scale Solution
dotted - GMS Fast and Slow Scale Solution

LATERAL-DIRECTIONAL DYNAMICS

As seen in the previous chapter, the lateral-directional motion along the entry trajectory is characterized by one oscillatory mode and two nonoscillatory modes. The two real roots (nonoscillatory modes) are degenerate cases. The spiral mode is unstable and will be an increasing exponential function. The Roll mode is stable and will be a decreasing exponential function. The Dutch-Roll mode, however, will have an

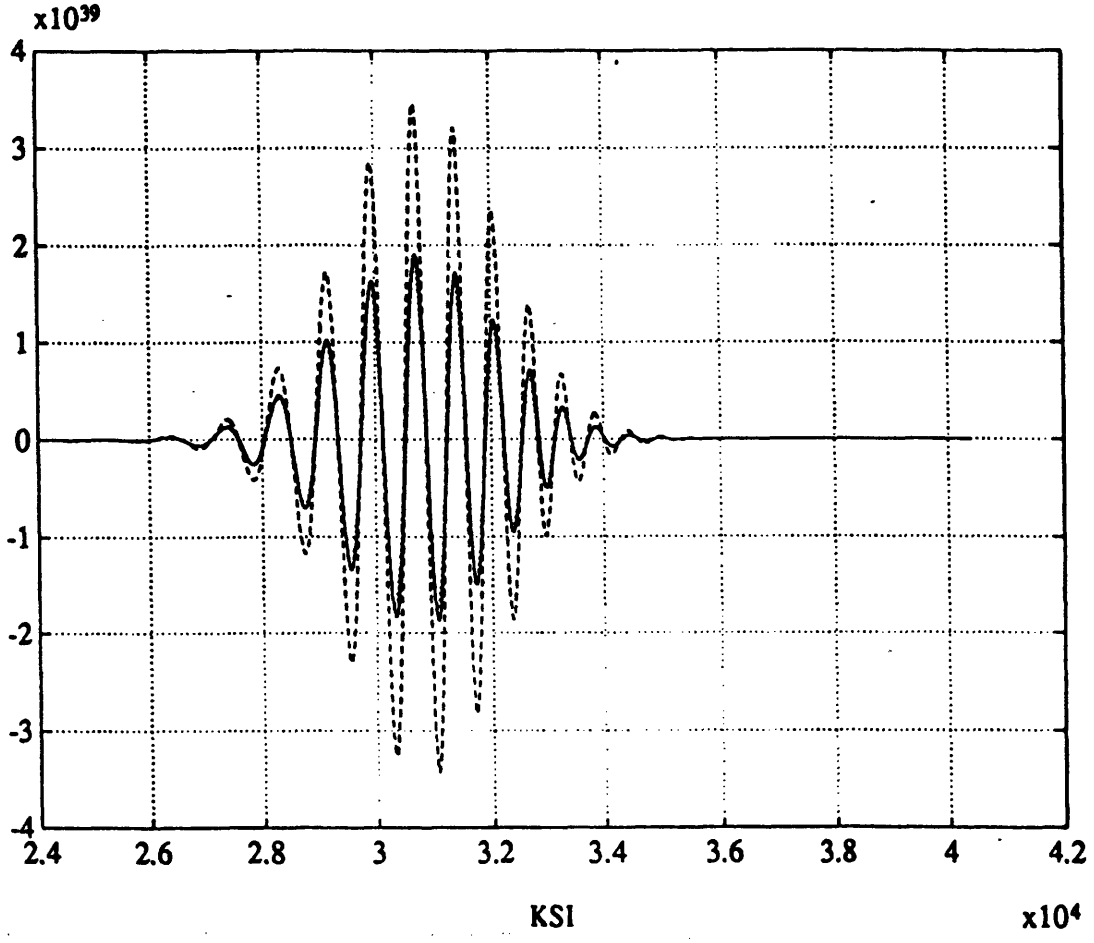

Figure 8.7 GMS Solutions to Dutch-Roll Mode
solid - Numerical Solution
dashed - GMS Fast Scale Solution
dotted - GMS Fast and Slow Scale Solution

oscillatory solution because of its complex roots. It can be evaluated in the same way as the longitudinal modes by constructing a second order equation and introducing the small parameter ε. The numerical and GMS solutions are shown in Figure 8.7. The response is initially an unstable oscillation consistent with complex roots in the right half plane. The amplitude of the oscillation initially increases. As the roots progress to the left half plane the response becomes a stable oscillation, and the amplitude begins to damp out. The GMS solutions for this mode are similar to those for the longitudinal modes. The GMS fast scale solution is seen to overshoot the numerical solution while the GMS fast and slow scale solution accurately predicts the Dutch-Roll motion of the GHAME vehicle.

The GMS approximations to each of the second order modes of motion have been seen to accurately predict the dynamics of the GHAME vehicle. These results have been extended by Ramnath [13] to the fourth order models describing longitudinal and lateral-directional motions. The fourth order differential equation is parameterized with ε according to the following equation

$$X^{(4)} + \frac{\omega_3 X^{(3)}}{\varepsilon} + \frac{\omega_2 X^{(2)}}{\varepsilon^2} + \frac{\omega_1 X^{(1)}}{\varepsilon^3} + \frac{\omega_0 X}{\varepsilon^4} = 0$$

The GMS solution is given by

$$X(\xi) = X_s(\xi) X_f(\xi)$$

where

$$X_f(\xi) = \left(C_1 \left[\exp\left(\int k_{Ar}(\xi) d\xi \right) \sin\left(\int k_{Ai}(\xi) d\xi \right) \right] + C_2 \left[\exp\left(\int k_{Ar}(\xi) d\xi \right) \cos\left(\int k_{Ai}(\xi) d\xi \right) \right] \right)$$

$$+ \left(C_3 \left[\exp\left(\int k_{Br}(\xi) d\xi \right) \sin\left(\int k_{Bi}(\xi) d\xi \right) \right] + C_4 \left[\exp\left(\int k_{Br}(\xi) d\xi \right) \cos\left(\int k_{Bi}(\xi) d\xi \right) \right] \right)$$

The root of one oscillatory mode is k_A and the other is k_B. The arbitrary constants are C_1, C_2, C_3 and C_4 which are determined by the initial conditions.

The results of simulation show that the analytical asymptotic solutions developed by the GMS method accurately predict the dynamics of the GHAME vehicle along the entry trajectory. They will be applied in the following chapter to stability and control analysis.

9. STABILITY AND CONTROL ANALYSIS

STABILITY CRITERION

Stability and control analysis is a primary application that comes from the understanding of aircraft dynamics. In the previous chapters, the motion of the GHAME vehicle was described by differential equations with time varying coefficients. The angle of attack dynamics were described by the unified equation developed by Vinh and Laitone. The longitudinal and lateral-directional motion were described by fourth order characteristic equations derived from Newton's Law. The roots of these were plotted as the vehicle moved along an entry trajectory. As mentioned earlier, the root locations are not sufficient to predict the stability of time varying systems. These systems can often exhibit counterintuitive behavior [10]. Therefore, asymptotic analytical solutions were developed using the GMS technique. From these solutions, the stability of the dynamics can be predicted and control laws can be developed. The GMS solution to a second order differential equation with one oscillatory mode was shown to be

$$X(\xi) = (\omega_1^2 - 4\omega_0)^{-1/4}\left(C_1\left[\exp\left(\int k_r(\xi)d\xi\right)\sin\left(\int k_i(\xi)d\xi\right)\right] + C_2\left[\exp\left(\int k_r(\xi)d\xi\right)\cos\left(\int k_i(\xi)d\xi\right)\right]\right)$$

From this solution a GMS stability criterion can be developed [10]. It can be concluded that the real part of the complex root must be in the left half plane to ensure stability.

$$k_r < 0$$

This would give a decaying exponential term in the solution and result in a damped oscillatory motion.

The results from the previous chapter which show the solutions to the equations of motion support this criterion for stability. The unified angle of attack motion has roots in the left half plane and is shown to have a stable oscillatory solution. Both modes of longitudinal motion have roots in the left half plane and are also shown to have stable oscillatory solutions. The Dutch Roll mode of the lateral-directional motion has roots that begin in the right half plane and move into the left half plane. The solution is consistent with the stability criterion determined above. It is initially an unstable oscillation which could reach a large magnitude. It then becomes a stable oscillation as the roots move into the left half plane and the amplitude decays.

FEEDBACK CONTROL

A control law can be developed for the Dutch Roll mode to ensure that the roots always lie in the left half plane. The Routh stability criterion, often used in linear time-invariant problems, can be extended by means of the GMS theory to apply to time-varying problems as well. It will be used to develop a feedback control law that will stabilize this mode. The Routh criterion tells us whether or not there are positive roots of a polynomial without actually solving for them. It states that the number of roots of the polynomial with positive real parts is equal to the number of changes in sign of the coefficients in the first column of the Routh array. See Etkin's Dynamics of Flight: Stability and Control for the details of this procedure [3].

The Routh stability criterion is only valid for constant coefficient differential equations but can be applied to this time varying problem

because of the stability criterion derived from the GMS solution. A sufficient condition for the stability of the GMS approximation is that the roots always lie in the left half plane. Therefore, the Routh criterion can be applied to this time varying problem to develop a control law. The general system equation is

$$k^2 + \omega_1 k + \omega_0 = 0$$

The Routh criterion results in two inequalities that would ensure stability

$$\omega_1 > 0 \qquad \omega_0 > 0$$

When both of these conditions are met the GMS solution is stable. Figure 9.1 shows both of these quantities as they vary along the trajectory. It is seen that ω_1 initially violates the stability criterion while ω_0 always lies within the prescribed boundary for stability.

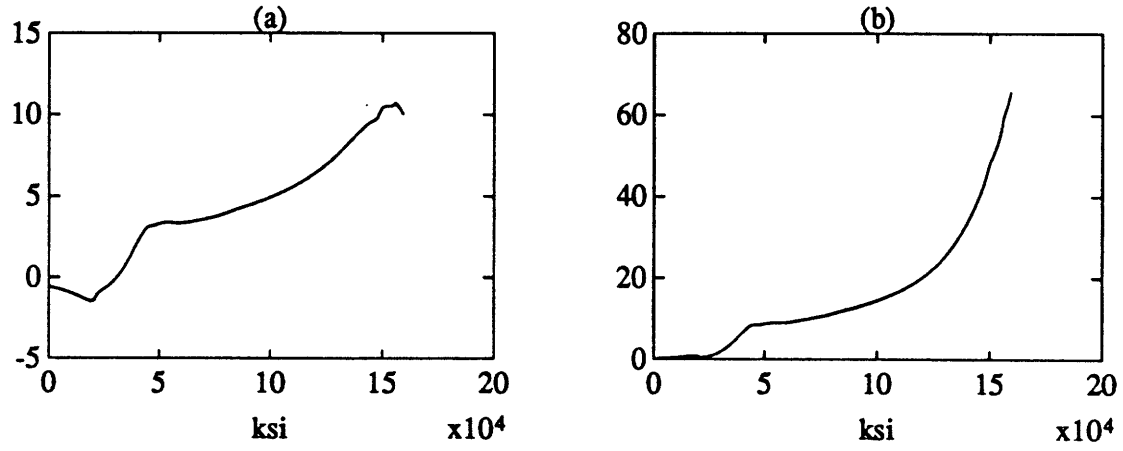

Figure 9.1 Coefficients of Dutch Roll Mode (a) ω_1 (b) ω_0

A feedback control law will be developed according to the block diagram in Figure 9.2 where K_1 is the feedback gain. Only the ω_1 coefficient needs to be modified since the condition on ω_0 is already satisfied. The

control law will modify the dynamics of the system and stabilize the response. The closed loop characteristic equation becomes

$$k^2 + (\omega_1 + K_1)k + \omega_0 = 0$$

The resulting Routh inequalities with feedback control are

$$\omega_1 + K_1 > 0 \qquad \omega_0 > 0$$

The ω_0 constraint was already shown to be satisfied over the entire trajectory. K_1 will be chosen to satisfy the constraint on ω_1.

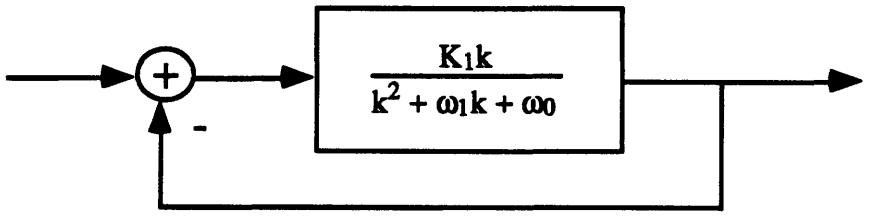

Figure 9.2 Feedback Control Block Diagram

The feedback gain was chosen to be a constant at K_1=2.5. This satisfies the inequality constraint on the ω_1 coefficient. Figure 9.3 shows the response of the Dutch Roll mode when the feedback is applied. The large spike of the uncontrolled response, shown in Figure 8.7, is removed by the feedback controller. The controlled response is shown to be a stable oscillation that is heavily damped.

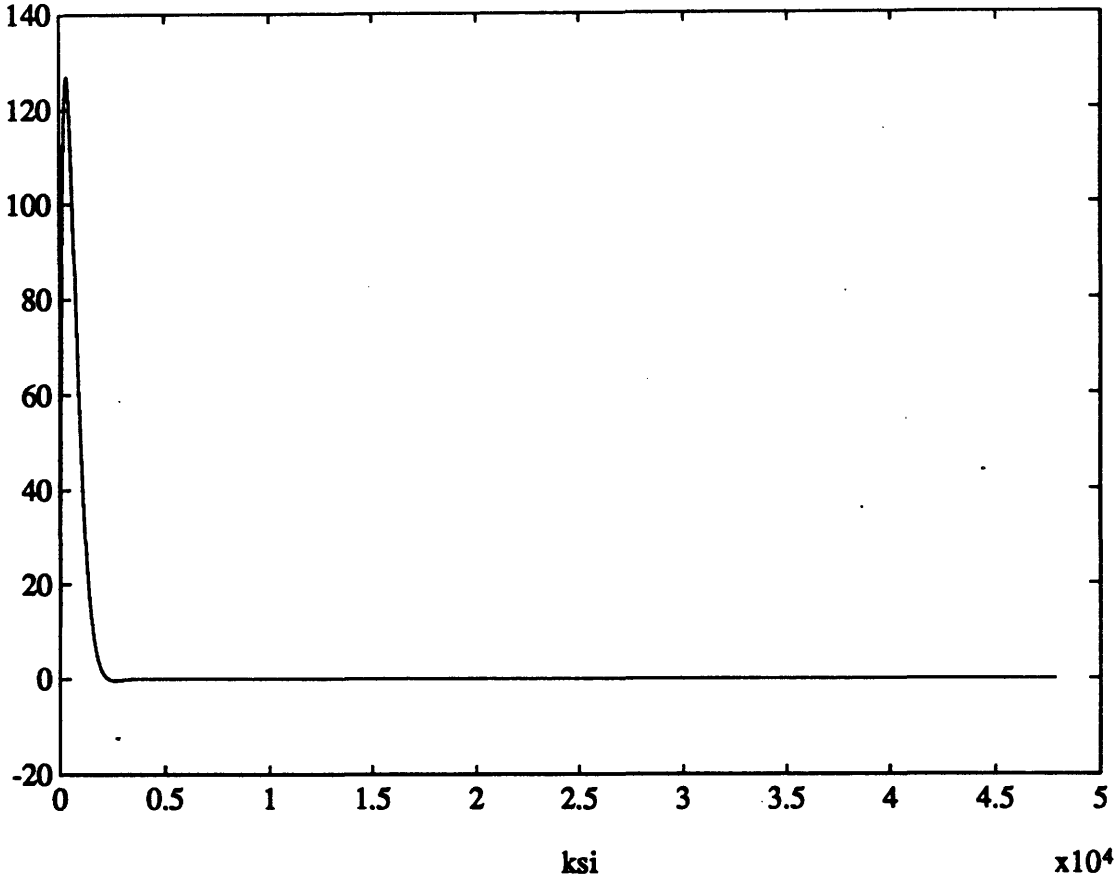

Figure 9.3 Dutch Roll Response With Feedback Control

10. SUMMARY AND CONCLUSIONS

SIMULATION

In this paper, the dynamics of a hypersonic vehicle (HSV) were analyzed along an entry trajectory using the asymptotic method of Generalized Multiple Scales (GMS). The rigid body equations and the general modes of aircraft motion were reviewed. A mathematical model describing the expected performance of future HSVs was provided by NASA called the Generic Hypersonic Aerodynamic Model Example (GHAME). A description of the GHAME vehicle was given along with its mass properties and aerodynamic data.

The model was used for computer simulation based on a table look-up method in which the stability derivatives of the vehicle were determined at discrete points along the trajectory. The GHAME vehicle is flown along a nominal entry trajectory used by the Space Shuttle which duplicates its interface conditions, vehicle constraints and trajectory parameters. A Fortran implementation of the shuttle entry guidance algorithm was adapted for MACINTOSH simulation of the GHAME vehicle.

GMS METHOD

The equations describing the motion of the GHAME vehicle result in a series of linear differential equations with variable coefficients. It is impossible to obtain exact solutions to such equations except in rare cases. Direct perturbation methods based on asymptotic analysis lead to nonuniformities in the approximate solutions to dynamic systems. The

technique of Generalized Multiple Scales (GMS) allows for the development of asymptotic solutions to linear and nonlinear differential equations with variable coefficients. These approximations are in an analytical form in terms of elementary functions and are uniformly valid over a wide range of the independent variable. The solutions are possible by considering the dynamics of the system to occur much faster than the changes in the coefficients of the model. The fast and slow parts of the dynamics are separated through an extension of the independent variable.

The coefficients of the equations describing the dynamics of the GHAME vehicle are recorded along the trajectory. The independent variable is changed from time to the distance traveled by the center of mass along the trajectory. The equations are parameterized in terms of a small parameter ε, and approximate solutions are determined using the GMS method. The equations analyzed include the unified equation describing angle of attack oscillations developed by Vinh and Laitone as well as the characteristic equations describing longitudinal and lateral-directional motion.

RESULTS

The trajectory was restricted to eliminate a small region where there might be complications in the solutions due to a possible turning point in the vicinity. The unified angle of attack dynamics of the GHAME vehicle was characterized by one oscillatory mode. The complex pair of roots began in the left half plane and increased in both frequency and damping as the vehicle moved along the trajectory. A reference solution to the dynamics was obtained through numerical integration. A "frozen"

approximation to the dynamics was obtained by holding the coefficients constant at their initial values and integrating. The reference solution was a damped oscillation which increased in both frequency and damping. The "frozen" approximation failed to predict the dynamics within the first quarter cycle of the oscillation. The GMS solution with only the fast dynamics accurately predicts the frequency of oscillation but overshoots the magnitude of the reference solution. The combined GMS solution with both fast and slow dynamics accurately predicts the entire dynamics of this motion.

The longitudinal motion of the GHAME vehicle was characterized by two oscillatory modes corresponding to the Phugoid and Short Period motion of aircraft. Each mode was isolated and then evaluated in the same manner described above. The Phugoid mode resulted in a low frequency and low damping oscillation while the Short Period mode was characterized by a high frequency and high damping oscillation. The results from the approximate solutions were the same as those from the unified angle of attack equation. The "frozen" solutions were inadequate approximations while the combined GMS solutions were able to accurately predict the dynamics of each mode.

The lateral-directional motion of the GHAME vehicle was characterized by three modes corresponding to the Roll, Yaw and Dutch Roll modes of motion. The Dutch Roll mode resulted in an oscillation that was initially unstable. It then became a stable oscillation as the amplitude damped out. The GMS combined solution was again shown to accurately predict the dynamics of this mode.

The analytical asymptotic solutions developed by the GMS method were shown to accurately predict the dynamics of the GHAME vehicle along

the entry trajectory. These approximate solutions lead to the development of a criterion which would ensure the stability of motion. The real part of the complex root must be in the left half plane for stability.

The solutions to the equations of motion confirm this criterion. Modes with roots in the left half plane were stable while those with roots in the right half plane were unstable. A feedback control law was then developed from this criterion to stabilize the oscillation of the Dutch Roll mode. A control gain was determined which produced a well damped oscillation. The unstable region of the Dutch Roll motion was eliminated by the feedback controller based on the stability criterion developed from the GMS solutions.

REFERENCES

1. Bowers, A. H. and K. W. Iliff, "A Generic Hypersonic Aerodynamic Model Example (GHAME) For Computer Simulation," NASA Ames Research Center, Dryden Flight Research Facility. Edwards, California. August 5, 1988.

2. Cox, R. N., Elements of Hypersonic Aerodynamics. Academic Press, New York. 1965.

3. Etkin, B., Dynamics of Flight: Stability and Control. 2nd ed. John Wiley & Sons, Inc., New York. 1982.

4. Harpold, J. C. and C. A. Graves Jr., "Shuttle Entry Guidance," AAS 78-147, AAS 25th Anniversary Conference, Houston, Texas, October 30 - November 2, 1978.

5. Feshchenko, S.F., N. I. Shkil, and L.D. Nikolenko, Asymptotic Methods in The Theory of Linear Differential Equations. American Elsevier Publishing Co., INC., New York. 1967.

6. McCallum, D., "Sliding Mode Control of GHAME Vehicle," Charles Stark Draper Laboratory, Cambridge, Mass.1990.

7. Nelson R. C., Flight Stability and Automatic Control. McGraw Hill, Inc., New York, 1989.

8. Paris, R. B. and A. D. Wood, Asymptotics of High Order Differential Equations. John Wiley & Sons, Inc., New York. 1986.

9. Ramnath, R. V., Class Notes "Introduction To Flight Vehicle Dynamics," MIT course 16.16 Fall 1989.

10. Ramnath, R. V., Class Notes "Advanced Flight Dynamics and Control," MIT course 16.17 Spring 1990.

11. Ramnath, R.V., "A Multiple Time Scales Approach to a Class of Linear Systems", Rep. No. AFFDL-TR-68-60, W.P. AFB, Dayton, Ohio. 1968.

12. Ramnath, R. V., J. K. Hedrick and H. M. Paynter. eds., Nonlinear System Analysis and Synthesis: Vol. 2-Techniques and Applications. The American Society of Mechanical Engineers. New York. 1980.

13. Ramnath, R.V. and G. Sandri, "A Generalized Multiple Scales Approach to a Class of Linear Differential Equations", J. M. A. A. Vol. 28, N0.2, pp. 339-364. 1969.

14. Ramnath, R. V. and P. Sinha, "On The Dynamics of The Space Shuttle During Entry Into Earth's Atmosphere," Charles Stark Draper Laboratory, Cambridge, Mass. November 1973.

15. Vinh, N. X. and Laitone, E. V., "Longitudinal Dynamic Stability of a Shuttle Vehicle", J. Astr. Sci. Vol. XIX, No. 5 pp. 337-363. March 1972.